

**LINEAR AND NON LINEAR VIBRATION RESPONSE OF THIN
ROTATING DISKS**

by

Ramin MohammadHasani Khorasany

B.Sc., Sharif University of Technology, Iran, 2002

M.Sc., Sharif University of Technology, Iran, 2004

A THESIS SUBMITTED IN PARTIAL FULFILMENT OF
THE REQUIREMENTS FOR THE DEGREE OF
DOCTOR OF PHILOSOPHY

in

THE FACULTY OF GRADUATE STUDIES

(Mechanical Engineering)

THE UNIVERSITY OF BRITISH COLUMBIA

(Vancouver)

Sept 2010

© Ramin MohammadHasani Khorasany

Abstract

Spinning disks have substantial applications in today's industries (e.g., saw mill industries). Developing a greater understanding the dynamics of spinning disks is a central topic for this thesis. Specifically, this thesis investigates the linear and nonlinear vibrations of spinning disks.

In some of the spinning disk applications, the disks may experience a rigid body translational degree of freedom. Having this degree of freedom can change the stability characteristics of spinning disks. Using analytical techniques and a two-mode approximation, the stability characteristics of elastically guided spinning disks having a rigid body translational degree of freedom are thus studied.

The effect of axisymmetric non-flatness on the frequency behaviour of spinning disks is also studied. The equations of motion are based on Von Karman plate theory. Assuming that the shape of initial runout is in the form of mode shapes with zero nodal diameters, the equations of motion are then discretized. Neglecting higher order terms, the equations are linearized and the effects of different levels of initial runout on the dynamics of spinning disks are thus studied.

Using experimental measurements, the effects of large deformations on the frequency behaviour and amplitude of response for the spinning disks are investigated. Disks with different thicknesses are used in this study. The disks were under the application of a space fixed external force which can produce different levels of nonlinearity. By measuring the disk displacement and conducting FFT analyses, the frequencies were measured for different levels of initial deflection.

In order to see how the geometrical nonlinear terms affect the frequency behaviour of spinning disks, the nonlinear governing equations are discretized and then solved to find the equilibrium solutions. By assuming a small perturbation around the equilibrium solution, the nonlinear equations of motion are linearized. Using the linearized form of the equations of motion, the effect of large deformations of the frequency characteristics of spinning disks is analyzed. The analytical results are then compared with the experimentally obtained results.

Table of Contents

Abstract.....	ii
Table of Contents	iii
List of Tables	vi
List of Figures.....	vii
List of Symbols	x
Acknowledgments	xiii
Dedication	xiv
Statement of Co-Authorship	xv
Chapter 1- Introduction	1
1.1. Background.....	1
1.2. Linear Theory of Vibration.....	2
1.2.1. Clamped Disks	3
1.2.2. Elastically Constrained Spinning Disks	7
1.2.3. Effects of Rigid Body Translation on the Dynamics of Spinning Disks	9
1.3. Nonlinear Theory of Vibration	10
1.3.1. Nonlinear Analysis and Basic Assumptions	10
1.3.2. Disk Initial Runout.....	12
1.3.3. Experimental Investigations on the Effects of Large Deformations	13
1.3.4. Numerical Investigations on the Effects of Large Deformations.....	14
1.4. Objective and Scope.....	16
1.5. References.....	19
Chapter 2- On the Effects of Rigid Body Translational Mode	25
2.1. Introduction.....	25
2.2. Linear Equations of Motion	26
2.3. Interaction Between a Backward Traveling Wave and Its Complex Conjugate with Rigid Body Translational Mode.....	28
2.4. Interaction Between a Forward or Backward or Reflected Traveling Wave with Rigid Body Translational Mode.....	32

2.5.	Conclusions.....	39
2.6.	References.....	40
Chapter 3- On the Effects of Initial Runout.....		42
3.1.	Introduction.....	42
3.2.	Formulation.....	43
3.3.	Solution Method.....	47
3.4.	Numerical Simulations.....	51
3.5.	Conclusions.....	62
3.6.	References.....	63
Chapter 4- Experimental Investigations on the Nonlinear Frequency Behavior		65
4.1.	Introduction.....	65
4.2.	Experimental Setup.....	66
4.3.	Experimental Results	68
4.3.1.	Disk #1 – 0.050” Thickness	68
4.3.2.	Disk #2 – 0.040” Thickness	75
4.3.3.	Disk #3 – 0.030” Thickness	78
4.4.	Conclusions.....	81
4.5.	References.....	83
Chapter 5- Analytical Investigations on the Nonlinear Frequency Behavior		85
5.1.	Introduction.....	85
5.2.	Formulation.....	87
5.3.	Linearization	91
5.4.	Numerical Analysis.....	95
5.4.1.	Stationary Disk.....	96
5.4.2.	Spinning Disk.....	98
5.5.	Conclusions.....	105
5.6.	References.....	107

Chapter 6- Summary and Conclusions	109
6.1. Summary and Conclusions.....	109
6.2. Recommendations for Future Work.....	113
6.3. References.....	114
Appendix A.	115

List of Tables

Table 3. 1. Ratio of disk deflection to its thickness at the outer rim when $W_{i0}^R = 100$	51
Table 3. 2. Comparison between the results of the proposed analysis and those predicted by ANSYS.....	52
Table 3. 3. Level of runout by which the frequencies of the oscillations of the (0,0) mode exceed those of the (0,2) and (0,3) modes	58
Table 3. 4. a_{mm}^ϕ for different modes and different forms of initial runout when $W_{i0}^R = 100$	59
Table 4. 1. Disk Dimensions and Flatness Indicators (inches)	67
Table 4. 2. Estimated Frequencies at Zero Speed (Hz); (0,2) Mode.....	72

List of Figures

Figure 1.1. Guided saw blade.....	1
Figure 1.2. Natural frequencies versus rotation speed	4
Figure 1.3. The (a) natural frequencies and (b) real part of the eigenvalues of an elastically constrained disk	8
Figure 1.4. The (a) natural frequencies and (b) real part of the eigenvalues of an elastically constrained disk having rigid body translational degree of freedom	9
Figure 1.5. Linear and nonlinear response of the blade at 1850 RPM for w/h when (a) $F=1$ N and (b) $F=10$ N	12
Figure 2. 1. A guided rotating disk with rigid body degrees of freedom.....	27
Figure 2. 2. Normalized natural frequencies of the guided disk (shown with the broken lines) versus normalized speed when (a) $k = 0.057$ and (b) $k = 2.85$. The solid lines show the normalized natural frequencies of the unguided disk..	32
Figure 2. 3. A general shape for $f(\omega, k)$ using the characteristics of a backward or forward traveling wave	34
Figure 2. 4. A typical plot of $f_1(\omega, k)$ (solid line) and $f_2(\omega, k)$ for a relatively small (dotted line) and large (dashed line) value of k when the discriminant of $f_2(\omega, k)$ is positive.....	36
Figure 2. 5. A typical plot of $f_1(\omega, k)$ (solid line) and $f_2(\omega, k)$ for a relatively small (dotted line) and large (dashed line) value of k when the discriminant of $f_2(\omega, k)$ is negative.....	37
Figure 2. 6. The interaction between the (0,2) mode of the clamped disk with rigid body translational mode when (a) $k = 1$, (b) $k = 2$, (c) $k = 5$, (d) $k = 10$, (e) $k = 10^4$ and (f) $k = 10^6$	38
Figure 3. 1. Non-dimensionalized oscillation frequencies versus non-dimensionalized rotation speed when the runout is zero (solid lines) and when $W_{00}^R = 100$ (broken lines).....	53

Figure 3. 2. Non-dimensionalized oscillation frequencies versus non-dimensionalized rotation speed when the runout is zero (solid lines) and when $W_{10}^R = 100$ (broken lines).....	54
Figure 3. 3. Non-dimensionalized oscillation frequencies of the stationary disk when the non-flatness is assumed to be in the shape of the (0,0) mode	55
Figure 3. 4. Non-dimensionalized oscillation frequencies of the stationary disk when the non-flatness is assumed to be in the shape of the (1,0) mode	56
Figure 3. 5. Non-dimensionalized oscillation frequencies of the stationary disk when the non-flatness is assumed to be in the shape of the (2,0) mode	56
Figure 3. 6. Non-dimensionalized oscillation frequencies of the stationary disk when the non-flatness is assumed to be in the shape of the (3,0) mode	57
Figure 3. 7. Change in the critical speed of the (0,2) Mode, assuming different shapes of runout (the legends show the shape of initial non-flatness).....	61
Figure 3. 8. Change in the critical speed of the (0,3) Mode, assuming different shapes of runout (the legends show the shape of initial non-flatness).....	61
Figure 3. 9. Change in the critical speed of the (0,4) Mode, assuming different shapes of runout	62
Figure 4. 1. The Experimental Setup	68
Figure 4. 2. Frequency Response of Disk #1 for Different Force Levels	73
Figure 4. 3. Disk 1- DC Displacement versus Speed (probe 3)	74
Figure 4. 4. Disk 1- Waterfall plot with white noise magnetic excitation ($w_0/h = 0.0$) in the run-up case	74
Figure 4. 5. Disk 1- DC amplitude at 3600 RPM at the location of four probes (shown with stars) and the (0,3) mode curve fitting (solid lines) when $w_0/h = 0.6$	75
Figure 4. 6. Frequency Response of Disk #2 for Different Force Levels	77
Figure 4. 7. Disk 2- DC Displacement versus Speed (probe 3).....	78
Figure 4. 8. DC displacement of disk #3, when $w_0/h = 0.5$ at all probes	79
Figure 4. 9. Frequency Response of Disk #3 for Different Force Levels	80
Figure 4. 10. Disk 3- DC Displacement versus Speed (probe 3).....	81
Figure 5. 1. Linear natural frequencies of the disk versus rotation speed.....	95

Figure 5. 2. The nonlinear frequencies of the backward (solid lines) and forward (broken lines) traveling waves of (a) (0,2), (b) (0,3), and (c) (0,4) modes of the stationary disk 97

Figure 5. 3. (a) The particular part of the stress function, (b) the nonlinear radial stress and (c) the nonlinear hoop stress along the normalized radial direction for three different angular directions when $w_0/h = 4$ 98

Figure 5. 4. Nonlinear frequencies of the spinning 0.05 in.-thick disk when $w_0/h = 0.1$, (a) numerical results (broken and solid lines show the linear and nonlinear results, respectively), (b) experimental results (run-up case) 101

Figure 5. 5. A comparison between the numerical and experimental results (run-up case) for the dc amplitude of oscillations when $w_0/h = 0.1$ at the location of the applied external force..... 101

Figure 5. 6. Nonlinear frequencies of the spinning disk when $w_0/h = 0.6$, (a) numerical results 102

Figure 5. 7. A comparison between the numerical and experimental results (run-up case) for the dc amplitude of oscillations when $w_0/h = 0.6$ 103

Figure 5. 8. Calculated linear (broken lines) and nonlinear frequencies (solid lines) of the spinning disk when $w_0/h = 2.0$ 104

Figure 5. 9. Dc amplitude of oscillation when $w_0/h = 2.0$ 104

List of Symbols

a	Inner radius of the disc
b	Outer radius of the disc
A_D	Disk area
c_1, c_2	Coefficients in the homogenous part of the stress function
C_1, C_2, C_3 and C_4	Coefficients of the in-plane stresses terms
C_{rr}, C_r, C_θ	Coefficients of the in-plane stresses terms in normalized equation
$C_{mn}^w, S_{mn}^w, c_1^w, c_2^w$	Time dependent generalized coordinates of the disc for the transverse deflection of the disk
D	Disk bending rigidity ($Eh^3/[12(1-\nu^2)]$)
E	Young's modulus
F	Applied external point force
G_w	Gyroscopic matrix
h	Disc thickness
i	Imaginary unit ($\sqrt{-1}$)
k	Stiffness of the spring
K_w	Stiffness matrix
m	Number of nodal diameters
M	Maximum number of nodal diameter in approximation function
n	Number of nodal circles
(n,m)	A mode with n and m nodal circles and diameters, respectively
N	Maximum number of nodal circles in approximation function
N_R	The number of axisymmetric modes with which the runout of the disk can be approximated
$p(r, \theta, t)$	External pressure acting on the disk surface
(r, θ, z)	Space-fixed polar coordinate system
(r_F, θ_F)	Radial and angular position of the external point force

(r^k, θ^k)	Radial and angular position of spring
$R_{mn}^w(r), \tilde{R}_{mn}^w(r)$	Mode shape in the radial direction for the disk deflection
R_{mn}^ϕ	Eigenfunctions of the stress function in the radial direction
S_{mn}^{ew}, C_{mn}^{ew}	Equilibrium solutions for the amplitude of the sin and cos waves of the transverse displacement
S_{mn}^ϕ, C_{mn}^ϕ	Amplitudes of the sin and cos waves in the stress function
$S_{mn}^{e\phi}, C_{mn}^{e\phi}$	Equilibrium solutions for the amplitude of the sin and cos waves of the stress function
S	Disk domain
t	Time
u	The net deflection of a non-flat disk
w	Displacement in z direction
w_0	The maximum deflection of the stationary disk at the outer rim caused by the application of air jet
\tilde{w}	The disk deflection at around its critical speed
w_0^R	The initial deformation (non-flatness) of the disk
W_{mn}	Eigenfunctions for the transverse displacement
W_{i0}^R	The amplitude of runout corresponding to $(i,0)$ mode
Z_0	Rigid body displacement in the z direction
$\alpha_1, \alpha_2, \alpha_3, \alpha_4$	Constants in the characteristics equation
$\delta(\cdot)$	Dirac delta function
δ_{ij}	Kronecker delta
$\delta()$	Dirac delta
Δ	Discriminant of the characteristics equation
$\phi(r, \theta, t)$	Stress function
ϕ^h	The homogenous part of the stress function
ϕ^p	The particular part of the stress function

ϕ_{mn}	Eigenfunctions for the stress function
η	The ratio of inner radius to outer radius of the disk (a/b)
λ, λ_{mn}^w	Eigenvalues for the transverse displacement
λ_{mn}^ϕ	Eigenvalues for the stress function
ν	Poisson's ratio
$\Theta_{mn}(\theta)$	Mode shape in the θ direction
ρ	Density
σ_r, σ_θ	Radial and hoop stress due to rotation
ω	Imaginary part of the eigenvalue
$\tilde{\omega}_{mn}$	The natural frequency of the disk in the inertial frame
Ω	Rotation speed

Acknowledgments

First and foremost I would like to pay special tribute to my supervisor, Prof Stanley Hutton for his technical guidance and support during research. I also would like to thank Prof Mohamed Gadala who has provided me with lots of helps during my PhD studies.

I am also grateful to my PhD committee members: Prof Farokh Sassani, Prof Carlos Ventura and Dr Bruce Lehmann for their helpful inputs and valuable discussions.

The supports from the University of British Columbia Graduate Fellowships are highly appreciated.

I also would to thank all of my friends all around the world who have helped and motivated me during my PhD studies.

Last, but not least, I would like to thank my parents, brothers and sisters for their invaluable supports. My special thanks go to my lovely wife, Sara, for her unlimited patience, love and encouragements that have made this work possible.

Dedication

To:

Endless supports and encouragements of my parents, brothers and sisters

To:

My wife, Sara

Statement of Co-Authorship

Ramin MohammadHasani Khorasany is the primary author of papers presented in this work. For all these works Mr Khorasany identified and proposed the research topic, performed the literature survey and research, analyzed the data, performed the simulations and prepared the manuscript under the supervision and direction of Prof Stanley Hutton.

All this work has been done completely during Mr Khorasany's PhD program. None of the papers presented in this work have received credit or presented in any other thesis work.

Chapter 1- Introduction

1.1. Background

Spinning thin disks can be found in many engineering applications. Common industrial applications include circular saws (Figure 1.1), turbine rotors, brake systems, fans, precision gyroscopes, and computer storage devices. Spinning disks may experience severe vibration which could lead to fatigue failure of the system.

A disk is usually defined as a thin, flat, circular plate. Hence, the analysis of spinning disks involves the theory of thin plates. The first step in investigating the vibrations of the spinning disk is to set up a mathematical model of the system. The aim is to set up a model that captures the essential physics of the problem.

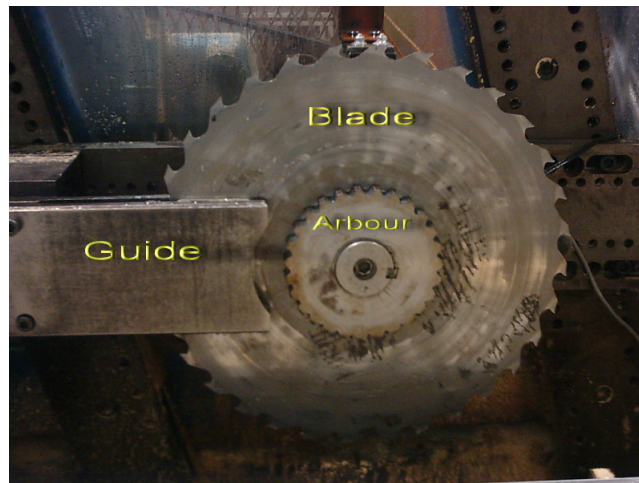


Figure 1.1. Guided saw blade

One of the most common applications of the rotating disks is in the saw mill industry. For several years, the blade that was used in this industry had a fixed inner boundary condition and free outer boundary condition. These types of saws are called “clamped” saws. Later on, less and less guided clamped saws were used in the saw mill industry. In the splined guided saw blades, the guide is composed of two flat pads in a space fixed point, and the blade rotates between the pads. The clearance between the pads and the blade is in the order of several thousandths of an inch. A combination of water and air is used to keep the blade cool and also to lubricate the blade. The splined saw blades have a rigid body translational degree of freedom. This degree of freedom can

substantially change the stability characteristics of spinning disks. Therefore, there is the need to study the effect of the rigid body translational degree of freedom on the dynamic behaviour of saw blades.

Saw blades in the mill industry have different sources of imperfections including those imperfections due to the initial non-flatness of the disk. The initial lack of flatness may change the frequency and critical speed behaviours of saw blades. Therefore in order to see how a non-flat saw blade performs at very high speeds, the effect of initial runout on the dynamics of spinning disks should be studied.

When saw blades are in the cutting modes, they experience external forces in the radial, tangential, and lateral directions. The lateral forces cause lateral deflections where, in some cases, these lateral deflections may change the dynamics of spinning disks at critical speed ranges. The effect of large deformations on the dynamics of spinning disks can be looked at both numerically and experimentally. Here, it will be determined how the frequency behaviour of spinning disks changes with regard to large deformations.

In the theory of vibrations for spinning disks, two different approaches have been taken. The first one utilizes linear theory where the effects of nonlinear terms are neglected; the second approach, nonlinear theory, instead takes those effects into account. The following sections introduce and discuss these two theories in detail.

1.2. Linear Theory of Vibration

In the approach based on the linear theory of vibration, the effect of higher order terms in the strain-displacement relations is neglected. Thus the resulting equations of motion are solely linear. The governing equation of transverse vibration of a spinning disk in terms of lateral displacement $w(r, \theta, t)$, with respect to a space fixed polar coordinate system shown with (r, θ) , can be written as [36]:

$$\rho h (w_{,tt} + 2\Omega w_{,t\theta} + \Omega^2 w_{,\theta\theta}) + D \nabla^4 w - \frac{h}{r} (\sigma_r r w_{,r})_{,r} - \frac{h}{r^2} \sigma_{,\theta} w_{,\theta\theta} = F(t) \quad (1.1)$$

Where D and ρ are the flexural rigidity and mass density of the plate respectively, $F(t)$ is the applied external load, a is the inner radius, b is the outer radius, h is its thickness, and Ω represents the angular velocity. σ_r and σ_θ the radial and tangential stresses, respectively, can be obtained through:

$$\sigma_r = \rho\Omega^2 \left(C_1 + \frac{C_2}{r^2} + C_3 r^2 \right) \quad (1.2a)$$

$$\sigma_\theta = \rho\Omega^2 \left(C_1 - \frac{C_2}{r^2} + C_4 r^2 \right) \quad (1.2b)$$

Two different disks with different boundary conditions are considered in this research work: the clamped disk and the splined disk. As mentioned above, for a clamped disk it is assumed that the inner boundary is fixed and the outer boundary is free. For the splined disk it is assumed that both of the boundaries are free. In the above equations C_1, C_2, C_3 and C_4 are constants that can be determined from the boundary conditions. For disks clamped at in the inner rim and free at the outer rim, the following equations can be used:

$$C_1 = \frac{1+\nu}{8} \frac{(\nu-1)a^4 - (3+\nu)b^4}{(\nu-1)a^2 - (1+\nu)b^2},$$

$$C_2 = \frac{1-\nu}{8} a^2 b^2 \frac{(\nu+1)a^2 - (3+\nu)b^2}{(\nu-1)a^2 - (1+\nu)b^2},$$

$$C_3 = -(3+\nu)/8,$$

$$C_4 = -(1+3\nu)/8.$$

For a splined disk with an idealized free-free boundary condition for both inner and outer rims C_3 and C_4 remain unchanged and C_1 and C_2 are:

$$C_1 = \frac{3+\nu}{8} (a^2 + b^2)$$

$$C_2 = -\frac{3+\nu}{8} a^2 b^2$$

The main focus of this work is to study the dynamics characteristics of the clamped disks. At first, brief discussions regarding the dynamical characteristics of clamped disks are presented. Following that considerations and discussions will be made of the effect of elastic constraints and the effects of elastic constraints and rigid body modes on the vibration characteristics of the spinning disks.

1.2.1. Clamped Disks

Figure 1.2 shows the natural frequencies of a disk calculated with respect to stationary coordinates with the inner and outer diameters of 6" and 17", respectively, and a thickness of 0.05". In this graph the modes are distinguished from each other by the

number of their nodal circles $-n-$ and also the number of their nodal diameters $-m-$ and shown as mode (n,m) . Corresponding to each mode there are two waves travelling around the disk. One travels in the direction of rotation (forward travelling wave) and the other travels in the opposite direction (backward travelling wave). It can be seen that natural frequencies of the backward and forward travelling waves of a mode are the same when the disk is stationary. Once the disk starts to spin, the natural frequency of the forward travelling wave increases and that of the backward travelling wave decreases as the rotation speed increases. It can be seen that for the modes having more than one nodal diameter a speed is reached at which the natural frequency of its backward travelling wave is zero. This speed is called the disk “critical speed.”

There has been a large body of research work concerning the dynamic characteristics of clamped spinning disks. Lamb et. al. [1] investigated the transverse vibration of a circular disk of uniform thickness rotating about its axis with constant velocity. Tian and Hutton [2] developed an analytical model for wood cutting of circular saws in order to understand the washboarding mechanism.

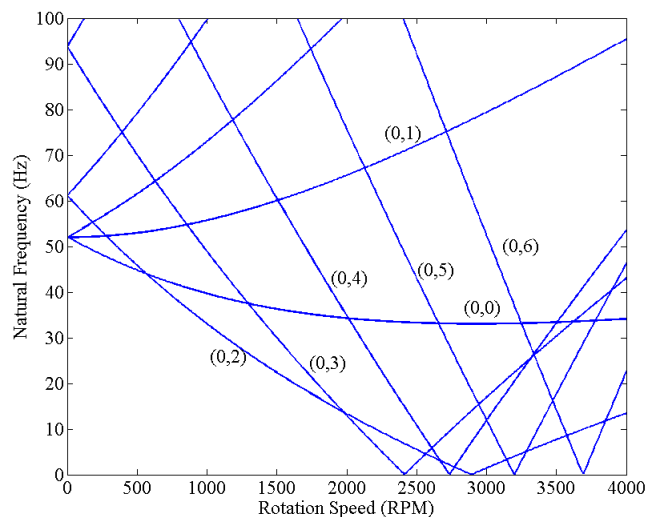


Figure 1.2. Natural frequencies versus rotation speed

Yu [3] presented a generalized Hamilton’s principle and the associated equation of motion for finite elastic deformation. By means of the generalized variational equation of motion, it is possible to deduce immediately the nonlinear equation of motion. He then employed the generalized variational equation of motion for the derivation of plate equations for both flexural and extensional motions. Mote [4] analyzed the free vibration

characteristics of centrally clamped, variable thickness disks by the Rayleigh-Ritz technique. Natural frequencies of transverse vibration were computed, taking into consideration rotational and thermal in-plane stress as well as purposely induced initial stress. Based on his analysis initial stresses can significantly raise the minimum disk natural frequency throughout a prescribed rotational and thermal environment. Vogel [5] derived the frequency determinants for various combinations of boundary conditions associated with the transverse vibrations of uniform annular plates. From these equations, he calculated the values of the resonant frequencies for various normal modes.

Chen [6] analyzed the forced response of a spinning disk under space fixed couples analytically using the eigenfunction expansion method. He considered a general couple on the disk surface as a superposition of two components. One of the components was pitching which was in the radial direction and the other one is a rolling component which is in the circumferential direction. He investigated the transient and steady state deflection of the disk. Nishio [7] investigated variations of the lateral vibration mode, the natural frequency, and the critical rotational speed of a slotted circular saw blade through both experiment and by numerical calculations.

J.-S. Chen performed numerous studies in the linear region of the rotating elastically constrained rotating disks. He [8] used the orthogonality properties that govern the modes to determine the certain derivative of modes with respect to a specified parameter. He then found the derivative of the natural frequencies of the system with respect to constraint parameters such as mass, damper, and stiffness. He [9] also used a series approximation to show that stress distribution induced by the friction effect from a fixed space source cannot affect the stability of the system. In other works ([10], [11] and [12]) he studied the effect of edge loads on the stability characteristics of a rotating disk.

DasGupta and Hagedorn [13] modelled the dynamics of spinning ring with a variable thickness external ring attached to it. They used von Karman plate theory to develop the equation of motion for the rotating disk with a ring attached to it. They found that a considerable change in the critical speed was achieved by designing an appropriate external ring. Kim and Renshaw [14] studied the effect of asymmetry of a spinning disk, using the finite element method. They investigated the effect of asymmetry on the natural frequencies of a rotating disk. Shen and Song [15] studied the effect of asymmetric

membrane stresses resulting from stationary in-plane edge loads. They used the method of multiple scales to study the stability of the disk subjected to stationary in-plane edge loads. Gupta et. al. [16] studied the asymmetric vibration of polar orthotropic circular plates. Adams [17] studied the effect of an elastic foundation on the critical speeds of a spinning disk. Eid et. al. [18] used Mindlin plate theory, which includes shear deformation and rotational inertia, to find the critical speeds of a spinning disk.

Parker and Mote [19] proposed a method for initially stressing the disk that can increase the natural frequencies of some of the modes simultaneously. In another work Parker and Mote [20] used a perturbation solution to analytically determine the eigensolutions of an annular plate. Young and Wu [21] studied the dynamic instability of a spinning disk with a periodically varying speed, subjected to a stationary in plane edge load. They used perturbation method to analyze the effect of varying speed on the vibration characteristics of the disk. Tian and Hutton [22] introduces a general approach which predicts the physical instability mechanism that take place when the rotating disk is in interaction with a fixed space constraint. They used a physical energy flux equation for the disk to explain its instability. Then they investigated the effect of conservative and non-conservative forces on the stability of the disk.

Shahab [23] used the Ritz method to investigate the transverse vibration of a disk with variable thickness. He developed a thick three dimensional element that includes the effect of rotary inertia and shear deformation for this purpose. Chung et. al. [24] investigated the effects of misalignment on the natural frequencies of a spinning disk. Huang, Wang, and Yap [25] studied feedback control of a rotating disk in an enclosure at flutter instability speed. They studied the effect of different gains on suppressing the transverse vibration of the disk. Gabrielson [26] presented the natural frequency of a disk with different boundary conditions and also different ratios of outer to inner diameter. Chen and Jhu [27] investigated the inplane vibrations of rotating disks. They studied the effect of clamping ration on the natural frequencies and critical speed of a rotating disk. Lee and Kim [28] developed direction frequency response functions for rotating disks. They then used this method to separate backward and forward travelling waves. Leissa, Laura, and Gutierrez [29] studied the free vibration of circular plates having non-uniform edge loads. They studied edge supports having translational and rotational flexibilities

which both vary in an arbitrary manner around the boundary of the disk. Gutierrez and Laura [30] studied the transverse vibration of a circular plate with a concentric circular support. Tandon, Rao, and Agrawal [31] performed experimental studies on vibration and noise generated by computer hard disk drives. Irie, Yamada, and Aomura [32] studied vibration and stability of radially stiffened annular plates subjected to in plane forces uniformly distributed at the edges by means of the energy method. Huang and Chou [33] studied the vibration feedback control of rotating disks. They used the root locus approach for an infinite number of poles and zeroes. By means of one sensor and one actuator they designed a feedback control algorithm for suppressing vibration in rotating disks. Chen [34] used a transfer function model to design a feedback control algorithm for suppressing vibration of rotating disks at sub- and super-critical speeds. He used one sensor and one actuator to implement his feedback control algorithm.

1.2.2. Elastically Constrained Spinning Disks

There are some applications for spinning disks such as in saw mill industry where they are elastically constrained. The constraint is generally modelled with a mass-spring-damper system. In this research work, only the spring component is considered. Figure 1.3 shows the natural frequencies and the real parts of eigenvalues of the elastically constrained spinning disk with the aforementioned dimensions. It is assumed that the spring stiffness is $4kN/m$ and that it is acting at the outer rim of the disk. It can be seen that the frequency characteristics of the spinning disk is different from the unconstrained disk.

Chen et. al. [35] studied the interaction of the mode at sub- and super-critical speeds. He categorized modal interactions to be four and he studied the effect of each of the constraint parameters on the stability of the system at sub- and super-critical speeds. He concluded that the interaction between the natural frequencies of backward and reflected travelling waves causes flutter type instability for an elastically constrained disk as shown in Figure 1.3.

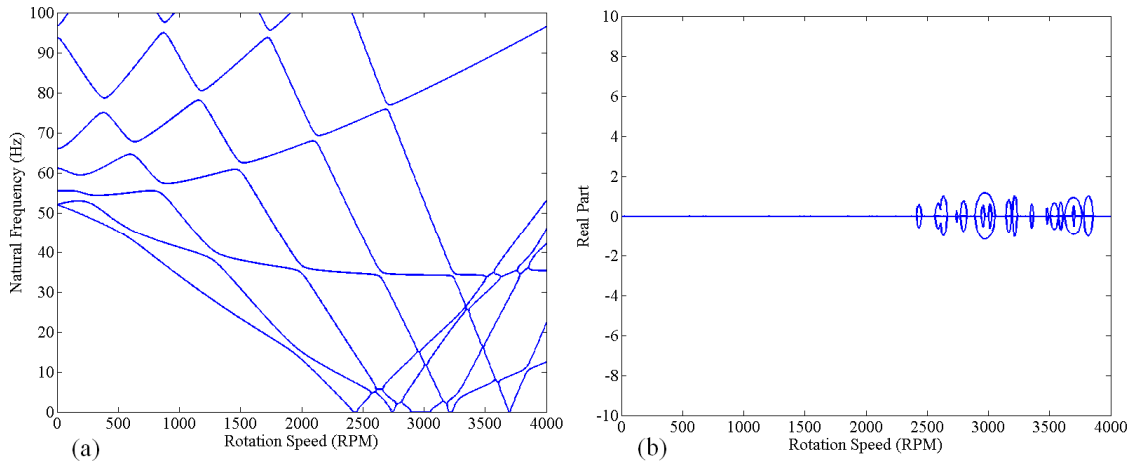


Figure 1.3. The (a) natural frequencies and (b) real part of the eigenvalues of an elastically constrained disk

When flutter instability happens, the real parts of eigenvalues have positive parts. Another source of instability for an elastically constrained disk is at the location of critical speed. This type of instability is called “divergence instability.” When the divergence instability occurs, there is one eigenvalue for the system with a zero imaginary part and a positive real part.

There are some works in the literature that studied the dynamics of elastically constrained spinning disks. Hutton, Chonan, and Lehmann [36] studied the dynamic response characteristics of rotating circular disks when subjected to the effect of forces produced by stationary spring guides. Young et al. [37] studied the free vibration of a rotation clamped disk under the constraint of an elastically fixed space oscillating unit. The unit he considered was composed of two parallel combinations of springs and dampers attached above and under a mass. He studied the flutter type instabilities imposed by these two units.

Ouyang and Mottershead [38] studied the instability of a transverse vibration of a disk excited by two sliders on each side of the disk. He modeled the sliders with a mass-spring-damper system. He considered the effect of friction due to movement of these two sliders on the disk which produces a fluctuating couple on the disk.

1.2.3. Effects of Rigid Body Translation on the Dynamics of Spinning Disks

Some of the spinning disk applications may have the rigid body translational degree of freedom along the axis of rotations. In this case, Eq. (1.1) should be modified such that it takes into account the effect of the rigid body translational degree of freedom.

When the rigid body translational degree of freedom is taken into account, the dynamic response of the disk will be different. Figure 1.4 shows the frequencies of the guided disk having the rigid body translational degree of freedom. Here it is also assumed that the spring stiffness is $4kN/m$ and it is acting at the outer rim of the disk.

Through comparison of Figure 1.4 with Figure 1.3 it can be seen that when the disk is elastically constrained with one spring the divergence instability does not occur at the location of critical speeds. Thus, the speed ranges at which the disk is stable are changed when the disk has a rigid body translational degree of freedom. It may be also noted that at sub-critical speeds there is a natural frequency which is constant and does not change with the speed. This natural frequency corresponds to rigid body motion. The interaction of this natural frequency with other natural frequencies may produce flutter instability.

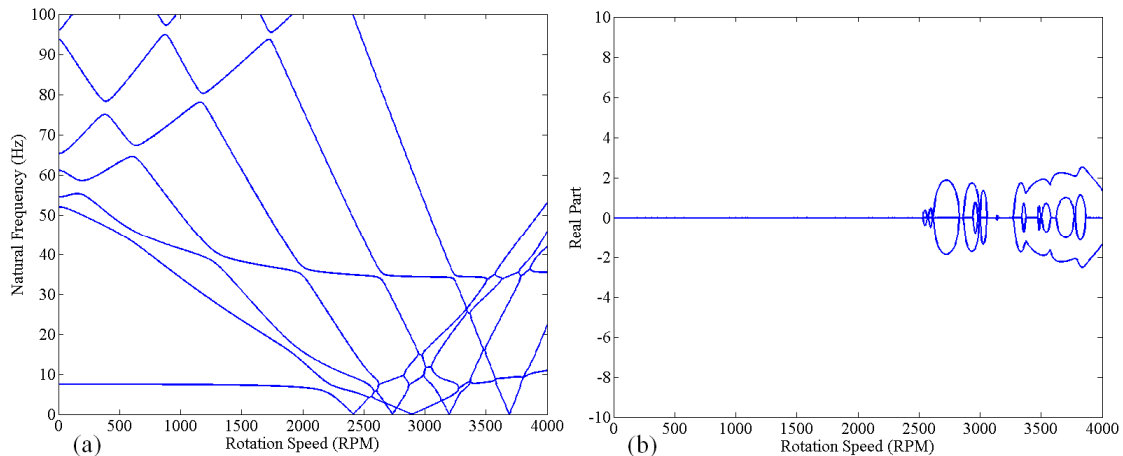


Figure 1.4. The (a) natural frequencies and (b) real part of the eigenvalues of an elastically constrained disk having rigid body translational degree of freedom

There has been a limited number of works that studied the effects of the rigid body translational degree of freedom on the stability characteristics of spinning disks. Yang [39] studied the vibration of spinning disks with translational and rotational rigid body motion. He considered the coupling effect between the rigid body motion and the annular

disk modal function. He showed that there is a stability region above the critical speed due to the coupling effect.

Mote [40] studied the effect of a collar (which was allowed to move freely on the arbor) on the stability of a guided rotating disk. Price [41] studied the dynamics of the plates with clamped-free boundary conditions and studied the effect of a rigid body translational mode on the dynamic response of rotating plates. Chen and Wong [42] used finite element analysis to study the effect of evenly fixed spaced springs on the divergence instability of a rotating disk having translational degrees of freedom. Chen [43] studied the effect of rigid body tilting on the natural frequencies of a rotating disk.

1.3. Nonlinear Theory of Vibration

In the nonlinear theory of vibration, the effect of higher order stress terms in strain-displacement relations are taken into account. Based on the linear theory of oscillations for spinning disks, disk deflection is unbounded at speeds corresponding to flutter or divergence instabilities. In fact, in these very cases, the disk deflection is beyond the validity range of linear equations of motion and it is necessary to use nonlinear equations for better predictions of the dynamics of spinning disks.

1.3.1. Nonlinear Analysis and Basic Assumptions

Nowinski [44] was amongst the first researchers to develop the nonlinear equations of motion for a spinning disk. He assumed the disk thickness to be much less than the outer radius. He also assumed that the disk is perfectly flat and is made of an isotropic material. He also assumed that the disk is free of any initial stress and that the effect of in-plane vibrations and rotary inertia are negligible. Based on these assumptions, he developed the nonlinear equations of motion of a spinning disk with speed Ω in the space-fixed polar coordinate system $((r, \theta))$ as:

$$\begin{aligned} \rho h \frac{\partial^2 w}{\partial r^2} + 2\Omega \frac{\partial^2 w}{\partial \theta \partial t} + \Omega^2 \frac{\partial^2 w}{\partial \theta^2} + D\nabla^4 w = L(w, \phi) + p(r, \theta, t) \\ - \frac{1}{2} \rho h \Omega^2 r^2 \nabla^2 w - \rho h \Omega^2 r \frac{\partial w}{\partial r}, \end{aligned} \quad (1.3)$$

$$\nabla^4 \phi = -\frac{1}{2} EhL(w, w) + 2\rho h(1-\nu)\Omega^2, \quad (1.4)$$

$$\nabla^4 = \frac{\partial^2}{\partial r^2} + \frac{1}{r} \frac{\partial}{\partial r} + \frac{1}{r^2} \frac{\partial^2}{\partial \theta^2},$$

where $p(r, \theta, t)$ is an external surface pressure, ϕ is the stress function and $L(w, \phi)$ is the operator that includes nonlinearities arising from the strain-displacement relations

$$L(w, \phi) = \frac{\partial^2 w}{\partial r^2} \frac{1}{r} \frac{\partial \phi}{\partial r} + \frac{1}{r^2} \frac{\partial^2 \phi}{\partial \theta^2} + \frac{\partial^2 \phi}{\partial r^2} \frac{1}{r} \frac{\partial w}{\partial r} + \frac{1}{r^2} \frac{\partial^2 w}{\partial \theta^2} - 2 \frac{1}{r} \frac{\partial^2 \phi}{\partial r \partial \theta} - \frac{1}{r^2} \frac{\partial \phi}{\partial \theta} \frac{1}{r} \frac{\partial^2 w}{\partial r \partial \theta} - \frac{1}{r^2} \frac{\partial w}{\partial \theta}.$$

Later on, Baddour et. al. [45] developed a full model of the nonlinear governing equations of motions considering the effects of in-plane displacements. The predicted responses based on the linear and nonlinear theories could be dramatically different. For instance, Figure 1.5 compares the linear and nonlinear analyses for a spinning disk with free-free boundary conditions at 1850 RPM. The rigid body degrees of freedom are taken into account in this analysis. The dimensions of the disk are the ones that are indicated previously. The disk was assumed to be elastically constrained by four linear springs at the radial locations: $0.58b, 0.88b$ and the angular positions $\theta_j = \pm 0.65, \pm 0.41 \text{ Rad}$. It can be seen that when the disk deflection is relatively small, e.g. $w/h < 1$, there is no significant difference in the amplitude of disk oscillations. It may be noted that in this case, there is a small difference in the oscillation frequencies. When the level of nonlinearity is high enough (e.g., $w/h > 1$), the predicted amplitudes of oscillations and their frequencies through nonlinear analyses are very different compared to those predicted by the linear analysis. Therefore, there is a need to investigate the effect of large deformations on the dynamical behavior of spinning disks. The effect of large deformations can either be investigated experimentally or analytically. Both of these methods are discussed in this work. Also, through the nonlinear form of the equations of motion, one can study the effect of initial disk runout on the frequency behaviour of the spinning disks.

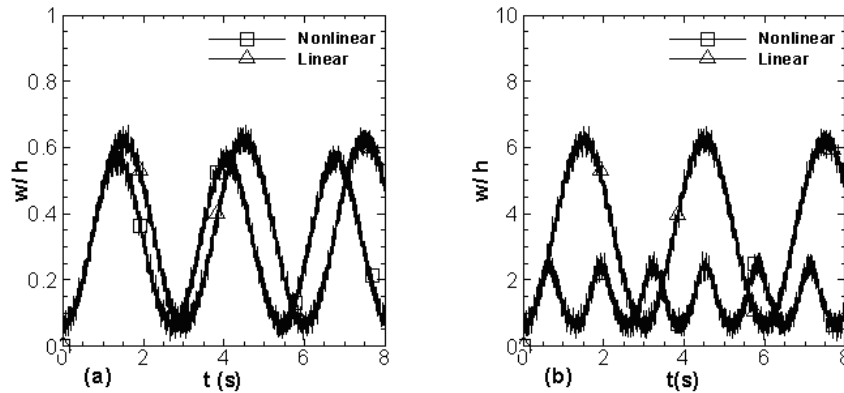


Figure 1.5. Linear and nonlinear response of the blade at 1850 RPM for w/h when (a) $F= 1 \text{ N}$ and (b) $F=10\text{N}$

1.3.2. Disk Initial Runout

Initial disk non-flatness can change the frequency characteristics of spinning disks. It also can change the critical speeds of spinning disks. To have a better understanding of the performance of spinning disks in real life applications, we have to know how the frequency and critical speed characteristics of spinning disks change when assuming the initial runout for them.

In order to study the effect of initial runout on spinning disk natural frequencies, one must use the governing equations of motion for initially non-flat spinning disks.

There have been a few studies in the literature that focus on the dynamics of non-flat disks. Jia [46] used the linear equation of motion to investigate the effect of runout on the vibration of a rotating disk. He approximated the runout of the blade with the summation of some modes having different nodal diameter numbers and then determined the deflection of the disk analytically. Since he used linear equations of motion, he could not study the effect of initial non-flatness on the frequency characteristics of spinning disks. Benson et al. [47] studied the effect of initial runout on the amplitude of oscillations, using both numerical and experimental techniques. At the same time, Carpino [48] investigated the effect of initial curvature of the dynamics of a disk rotating near a rigid surface.

While the aforementioned studies employed linearized equations of motion, other literature studies have considered the effect of geometrical nonlinear terms on the response of a non-flat spinning disk. Chen et al. [49] used the nonlinear governing

equations of motion to investigate the impact of symmetrical initial runout on the amplitude of spinning disk deflection. He concluded that depending on the shape and level of initial non-flatness, the disk may snap from one side to another. To verify his results, he used a warped disk with an initial level of non-flatness almost eight times higher than the disk thickness. In another work, Chen et al. [50] used the nonlinear equations of motion to consider an unsymmetrical initial non-flatness for the disk. In this paper, he studied the effect of unsymmetrical terms on the snapping speed while the disk was spinning.

1.3.3. Experimental Investigations on the Effects of Large Deformations

As it was mentioned earlier, large deformations may substantially change the vibration characteristics of spinning disks. Large deformations can change the amplitude of disk oscillations and they can also modify the frequency characteristics of spinning disks. In most of the experimental research work available in the literature, the amplitude response of spinning disks has been investigated experimentally.

Tobias and Arnold [51] investigated the effect of disk imperfections on the dynamic behavior of spinning disks. In their studies, they conducted experiments on the amplitude response of a spinning disk in the region of its critical speeds while subjected to a space fixed external force. They observed that a stationary wave develops in the region of a critical speed and collapses sometime after the critical speed. They did not consider the effect of large deformations on the frequency response characteristics of the disks that were tested. In another work [52], Tobias studied the large vibrations of stationary disks. He was able to record phase and amplitude jumps while the disk was being excited with a frequency close to one of its natural frequencies.

Thomas et. al. [53] measured the amplitude response of an imperfect stationary disk. Due to the presence of imperfections, there were two different configurations associated with each mode. He was able to measure the amplitude response of each configuration and compare them with analytical predictions. Raman and Mote [54] conducted experiments to study the behaviour of an imperfect spinning disk near its critical speeds. In their experimental work they were able to observe the existence of a critical speed for very small disk deflections.

In all of the aforementioned studies, the amplitude response of spinning disks has been studied. There are a few investigations in the literature that are concerned with the effect of large deformations on the frequency behaviour of spinning disks. D'Angelo and Mote [55] were amongst the first researchers to measure the oscillation frequencies of a spinning disk having large deformations. They noted that at supercritical speeds, the measured frequency of backward travelling waves maintain a constant level.

Raman et. al. [56] investigated experimentally the post-flutter frequency response of spinning disks. They recorded sudden jump and drops in the frequency response of the disks tested. Also, they noticed that the frequency response of the backward travelling wave of one of the modes was nearly constant over a specific speed region.

Namchelo and Raman [57] studied the vibrations of a spinning disk in a gas-filled enclosure. More recently, Jana et. al. [58] conducted experiments to investigate the aeroelastic phenomena of a disk rotating in air. They measured the amplitude and frequency responses of a spinning disk and noticed jumps and drops in the frequency response. They also reported that, in some supercritical speed ranges, a frequency lock-in phenomenon occurred.

1.3.4. Numerical Investigations on the Effects of Large Deformations

There has been an exhaustive amount of research work that explore the effects of geometrical nonlinear terms on the dynamics of spinning disks.

Jana and Raman [59] investigated the nonlinear dynamics of a flexible spinning disk coupled to a precompressed spring. They studied large amplitude wave motions and their stability using the averaging method. Chen [60] also studied the steady-state deflection of a rotating disk in the neighbourhood of its critical speed and found that after surpassing the critical speed there are three steady state solutions to the nonlinear equation of motion and only one of them is stable in the presence of space-fixed damping.

Nayfeh, Jilani, and Manzione [61] used the method of multiple scales to investigate the transverse nonlinear vibrations of a centrally clamped rotating circular disk. Chen [62] used the multiple scales method to investigate the internal resonance between a pair of forward and backward modes of a spinning disk under space fixed pulsating edge loads. Touze et al. [63] studied the nonlinear oscillations of a stationary disk with

imperfections. They also examined the coupling between preferential configurations and investigated its effect on the travelling wave components in the response.

Yang and Hutton [64] used polynomial expansion functions as the approximation function in Galerkin's method to solve the nonlinear equations of motion for thin rotating disks. Luo and Mote [65] used a new plate theory to study the effect of large amplitude displacements on the frequency behaviour of spinning disks. Based on energy principles they calculated the frequencies of a spinning disk with consideration of the effect of nonlinear terms.

Arafat, Nayfeh, and Faris [66] studied the behaviour of an annular disk subjected to axisymmetric in-plane thermal load with a clamped-clamped boundary condition. They investigated the effect of thermal loads on the natural frequencies of a stationary disk and found that, depending on the thermal load, there may be a three-to-one combination internal resonance between the modes having the same number of nodal diameters.

Arafat and Nayfeh [67] studied a three-to-one internal resonance between the first and second axisymmetric modes of an annular disk with a clamped-clamped boundary condition, which was subjected to an external force and a thermal load. They used multiple scales to find the governing equations for the amplitudes and phases of the responses. Arafat and Nayfeh [68] used von Karman plate theory to study the combination of internal resonance for a thermally loaded annular plate subjected to harmonic excitation near primary resonance of one of the modes with a clamped-clamped boundary condition. Chen, Hua, and Sun [69] used von Karman's plate theory to investigate the secondary resonance of a rotating disk under space fixed force. Heo, Chung, and Choi [70] used a finite element method to study the time domain response of a rotating disk misaligned from its axis of symmetry. In their analysis they considered both inplane and out of plane deformations of the disk. Raman and Mote [71] studied the large amplitude vibration of a rotating disk with imperfections near the critical speed.

Manziona and Nayfeh [72] studied the transverse vibrations of a circular spinning disk with uniform thickness subjected to a space fixed spring-mass-dashpot system. They used the method of multiple scales to find the nonlinear coupled governing equations of the motion and they studied the stability of the equilibrium solutions. Jalali and Angoshtari [73] used a Hamiltonian formulation to study the dynamics of forced spinning

disks. Using a Poincare map, they showed that a one mode approximation of rotating disks may have chaotic behaviour. Also they studied the effect of structural damping and showed the existence of asymptotically stable limit cycles for the damped system.

1.4. Objective and Scope

In this thesis, the vibration characteristics of spinning disks are investigated. This research work aims to examine the linear and nonlinear vibration characteristics of spinning disks with applications to the saw mill industry.

As was mentioned above, for some of the saw mills industries saw blades are not constrained in the inner rim and may have a rigid body translational degree of freedom. Thus, it is important to determine how the rigid body translational degree of freedom might affect the dynamics stability of saw blades at supercritical speeds.

There are several sources of imperfections in real saw blades. One such source is the imperfection due to a lack of flatness. These types of imperfections can change the modal stiffness characteristic of a saw blade. As such, they can change the frequency and critical speed behaviour of saw blades. Therefore, in order to have a better understanding of the dynamics of real saws, there will be a discussion on the effect of imperfections on the frequency and critical speed behaviour of spinning disks. Runouts can be axisymmetric or unsymmetrical. As a first step, the axisymmetric case is investigated in this work.

Real saw blades in cutting modes experience the application of radial, tangential, and lateral cutting forces. The lateral forces produce lateral deflections and when the lateral deflection is large compared to its thickness (e.g., greater than 0.3 of its thickness) the frequency and critical speed behaviour of saw blades change. This change is especially more noticeable at supercritical speeds. Therefore, the objective of this research work is to first study the effects of the rigid body translational degree of freedom, initial non-flatness, and large deformations on the dynamics of spinning disks. To meet these general objectives, the approach taken in this thesis consists of the following sub-objectives:

To understand the stability mechanics of a guided rotating disk with rigid body translational mode. The linear theory will be used to study the effect of rigid body modes on the stability characteristics of an elastically constrained rotating disk.

To study the effect of symmetrical non flatness on the frequency response of an elastically constrained disk. Also the effect of such these imperfections on the critical speeds of different modes are of major concern.

To experimentally investigate the amplitude and frequency characteristics of spinning disks under the application of a space fixed external force.

To analytically investigate the effect of nonlinear terms on the frequency response of a rotating disk using a linearization method. The aim is to study the effect of the level of nonlinearity on the forced frequencies of a rotating disk.

This thesis is presented in six chapters. In Chapter 2 a discussion on the linear model prediction for the stability of the disk is made. The linear equations of motion coupled with the rigid body translational mode are used to investigate the stability characteristics of an elastically constrained disk. The effect of the rigid body mode on the stability characteristics of a spinning disk is studied. Generally there are three types of interaction between the rigid body translational mode and bending modes: the rigid body translational mode may have interactions with a forward, backward, or reflected wave. The stability characteristics of the disk at the speeds corresponding to these types of interactions are studied. Also, a one mode approximation model around the critical speed is utilized to study the effect of the rigid body translational mode on the divergence instability of the disk.

Chapter 3 is concerned with the effect of non-flatness on the frequency response of a spinning disk assuming symmetric non-flatness. Since the non-flatness is assumed to be axisymmetric, the equations of motion can be expressed in an inertial frame. The non-flatness is assumed to be expressed as a summation of the eigenfunctions of the modes with a zero number of nodal diameters. As an approximation, the effect of higher order terms in the nonlinear equations of motion is neglected. Using this assumption the particular solution for the stress function is found from the compatibility relation. Substituting the stress function into the governing equation of motion and utilizing Galerkin's method while neglecting higher order terms, a linearized system of equations is found. Using the obtained linear system, the effect of symmetrical non-flatness on the frequency response of an elastically constrained spinning disk is investigated.

Chapter 4 is concerned with the effects of large deformations on the amplitude and frequency characteristics of spinning disks. This chapter describes attempts made to experimentally study the effects of nonlinear terms on the dynamics of spinning disks under the applications of space fixed external forces. Three disks with the same inner and outer radii and different thicknesses were used. Different levels of force are applied to these three disks and their amplitudes of oscillation and frequencies were measured.

Chapter 5 is primarily concerned with the effect of nonlinear terms on the forced frequency response of a disk using the linearization method. Using Galerkin's method, the nonlinear equations of motion are discretized. The equilibrium solution for a spinning disk under the application of a space fixed external force is found. Then, the nonlinear equations of motion are linearized around that equilibrium solution to obtain a linearized system of equations of motion. These linearized equations of motion are used to study the effect of different levels of nonlinearity on the frequency response of a rotating disk.

Finally, Chapter 6 presents the conclusions and suggestions for future investigations on this subject.

1.5. References

- [1] Lamb, H., and Southwell, R.V., 1921, "The Vibration of Spinning Disk," Proc R Soc Lond 99, pp. 272-280.
- [2] Tian, J.F., and Hutton, S.G., 2001, "Cutting-Induced Vibration in Circular Saws," Journal of Sound and Vibration, 242(5), pp. 907-922.
- [3] Yu, Y.Y., 1964, "Generalized Hamilton's Principle and Variational Equation of Motion in Nonlinear Elasticity Theory," Journal of the Acoustical Society of America, 36, pp. 111-120.
- [4] Mote, C.D., 1965, "Free Vibration of Initially Stressed Circular Plates," Journal of Engineering for Industry, 87, pp. 258-264.
- [5] Vogel, S.M., and Skinner, D.W., 1965, "Natural Frequencies of Transversely Vibrating Uniform Annular Plates", ASME Journal of Applied Mechanics, 32, pp. 926-931.
- [6] Chen, J.S., Hsu, C.M. , 1997, "Forced Response of a Spinning Disk Under Space-Fixed Couples," Journal of Sound and Vibration, 206(5), pp. 627-639.
- [7] Nishio, S., and Marui, E., 1996, "Effect of Slots on the Lateral Vibration of a Circular Saw Blade," International Journal of Machine Tools and Manufacture, 36(7), pp. 771-787.
- [8] Chen, J.S., and Bogy, D.B., 1992, "Effects of Load Parameters on the Natural Frequencies and Stability of a Flexible Spinning Disk With a Stationary Load System," Journal of Applied Mechanics, 59, pp. S230-S235.
- [9] Chen, J.S., and Bogy, D. B., 1993, "The Effects of a Spaced-Fixed Friction Force on the In-Plane Stress and Stability of Transverse Vibrations of a Spinning Disk," ASME Journal of Applied Mechanics, 60(3), pp. 646-648.
- [10] Chen, J.S., 1994, "Stability Analysis of a Spinning Elastic Disk Under a Stationary Concentrated Edge Load," ASME Journal of Applied Mechanics, 61, pp. 788-792.
- [11] Chen, J.S., 1996, "Vibration And Stability of a Spinning Disk Under Stationary Distributed Edge Loads," ASME Journal of Applied Mechanics, 63, pp. 439-444.
- [12] Chen, J.S., 1997, "Parametric Response of a Spinning Disk Under Space-Fixed Pulsating Edge Loads," ASME Journal of Applied Mechanics, 64, pp. 139-143.

- [13] DasGupta, A., and Hagedorn, P., 2005, "Critical Speeds of a Spinning Thin Disk With an External Ring," *Journal of Sound and Vibration*, 283, pp. 765-779.
- [14] Kim, H.R., and Renshaw, A.A., 1998, "Asymmetric, Speed Dependent Tensioning of Circular Rotating Disks," *Journal of Sound and Vibration*, 218, pp. 65-80.
- [15] Shen, I. Y., and Song, Y., 1996, "Stability and Vibration of a Rotating Circular Plate Subjected to Stationary In-Plane Edge Loads," *ASME Journal of Applied Mechanics*, 63, pp. 121-127.
- [16] Gupta. U.S., and Ansari, A.H., 1998, "Asymmetric vibrations and elastic stability of polar orthotropic circular plates of linearly varying profile," *Journal of Sound and vibration*, 215, pp. 231-250.
- [17] Adams, G., 1987, "Critical Speeds for a Flexible Spinning Disk," *International Journal of Mechanical Sciences*, 29 (8), pp. 525-531.
- [18] Eid, H., Adams, G.G., 2006, "Critical speeds and the response of a spinning disk to a stationary load using Mindlin plate theory," *Journal of Sound and Vibration*, 290, pp. 209-222.
- [19] Parker. R.G., and Mote, C.D., 1991, "Tuning of the Natural Frequency Spectrum of a Circular Plate by In-plane Stress, *Journal of Sound and Vibration*, 145, pp. 95-110.
- [20] Parker. R.G., and Mote, C.D., 1996, "Exact Perturbation for the Vibration of Almost Annular or Circular Plates," *Journal of Vibration and Acoustics*, 118, pp. 436-445.
- [21] Young, T. H., and Wu, M. Y., 2004, "Dynamic Stability of Disks with Periodically Varying Spin Rates Subjected to Stationary In-Plane Edge Loads," *Journal of Applied Mechanics*, 71, pp. 450-458.
- [22] Tian, J., and Hutton, S.G., 1999, "Self Excited Vibration in Flexible Rotating Discs Subjected to Transverse Interaction Forces – A General Approach," *ASME Journal of Applied Mechanics*, 66, pp. 800-805.
- [23] Shahab, A.A.S., 1993, "Finite Element Analysis for the Vibration of Variable Thickness Discs," *Journal of Sound and Vibration*, 162, pp. 67-88.

- [24] Chung, J.T., Heo, J.W., and Han, C.S., 2003, "Natural frequencies of a flexible spinning disk misaligned with the axis of rotation," *Journal of Sound and Vibration*, 260, pp. 763-775.
- [25] Huang, X.Y., Wang, X., and Yap, F.F., 2004, "Feedback Control of Rotating Disk Flutter in an Enclosure," *Journal of Fluids and Structures*, 19, pp. 917-932.
- [26] Gabrielson, T.B., 1999, "Frequency Constants for Transverse Vibration of Annular Disks," *Journal of Acoustical Society of America*, 105 (6) , pp. 3311-3317.
- [27] Chen, J.S., and Jhu, J.L., 1996, "On the In-Plane Vibration and Stability of a Spinning Annular Disk," *Journal of Sound and Vibration*, 195(4), pp. 585-593.
- [28] Lee, C.-W., and Kim, M.-E., 1995, "Separation and Identification of Travelling Wave Modes in Rotating Disk via Directional Spectral Analysis," *Journal of Sound and Vibration*, 187, pp. 851-864.
- [29] Leissa, A.W., Laura, P.A., and Guiterez, R.H., 1979, "Transverse Vibrations of Circular Plates Having Nonuniform Edge Constraints," *Journal of the Acoustical Society of America*, 66(1), pp. 180-184.
- [30] Gutierrez, R. H., and Laura, P. A. A., 2000, "Transverse Vibrations of a Circular Plate Polar Anisotropy with a Concentric Circular Support," *Journal of Sound and Vibration*, 231, pp. 1175-1178.
- [31] Tandon, N., Rao, V.V.P., and Agrawal, V.P., 2006, "Vibration and Noise Analysis of Computer Hard Disk Drives," *Journal of the International Measurement Confederation*, 39, pp. 16-25.
- [32] Irie, T., Yamada, G., and Aomura, S., 1982, "Vibration And Stability Of Stiffened Annular Plates," *Journal of Acoustical Society of America*, 72, pp. 466-471.
- [33] Huang, C.C., and Chou, R.J., 2000, "Vibration Control of a Rotating Disk," *Mechanical Systems and Signal Processing*, 14, pp. 151-165.
- [34] Chen, J.S., 2003, "Vibration Control of a Spinning Disk," *International Journal of Mechanical Sciences*, 45, pp. 1269-1282.
- [35] Chen, J. S., and Bogy, D.B., 1992, "Mathematical Structure of Modal Interactions in a Spinning Disk-Stationary Load System," *American Society of Mechanical Engineers Journal of Applied mechanics*, 59, pp. 390-397.

- [36] Hutton, S.G., Chonan, S., and Lehmann, B.F., 1987, "Dynamic Response of a Guided Circular Saw," *Journal of Sound and Vibration*, 112, pp. 527-539.
- [37] Young, T.H., and Lin, C.Y., 2006, "Stability of a Spinning Disk Under a Stationary Oscillating Unit," *Journal of Sound and Vibration*, 298, pp 307-18.
- [38] Ouyang, H., and Mottershead, J. E. , 2003, "A Moving-Load Model for Disc-Brake Stability Analysis," *Journal of Vibration and Acoustics*, 125, pp. 753-758.
- [39] Yang, S.M., 1993, "Vibration of a Spinning Annular Disk with Coupled Rigid-Body Motion," *Journal of Vibration, Acoustics*, 115, pp. 159-164.
- [40] Mote, C.D., 1977, "Moving Load Stability of a Circular Plate on a Floating Central Collar," *Journal of Acoustical Society of America*, 61, pp. 439-447.
- [41] Price, K.B., 1987, "Analysis of the Dynamics of Guided Rotating Free Center Plates," Ph.D. Dissertation, University of California, Berkeley.
- [42] Chen, J.S., and Wong, C.C., 1995, "Divergence Instability of a Spinning Disk with Axial Spindle Displacement in Contact with Evenly Spaced Stationary Springs," *Journal of Applied Mechanics*, 62, pp. 544-547.
- [43] Chen, J.S., and Bogy, D.B., 1993, "Natural Frequencies and Stability of a Flexible Spinning Disk-Stationary Load System With Rigid Body Tilting," *Journal of Applied Mechanics*, 60, pp. 470-477.
- [44] Nowinski, J.L., 1964, "Nonlinear Transverse Vibrations of a Spinning disk," *Journal of Applied Mechanics*, 31, pp. 72-78.
- [45] Baddour, N., Zu, J.W, 2001, "A revisit of spinning disk models. Part I: Derivation of equations of motion," *Applied Mathematical Modelling*, 25, 7, pp. 541-559
- [46] Jia, H. S., 2000, "Analysis of Transverse Runout in Rotating Flexible Disks by Using Galerkin's Method", *International Journal of Mechanical Sciences*, 42, pp. 237-248.
- [47] Benson, R.C., and Cole, K. A., 1991, "Transverse Runout of a Nonflat Spinning Disk," *Tribology Transactions*, 34, pp. 545-552.
- [48] Carpino, M., 1991, "The Effect of Initial Curvature in a Flexible Disk Rotating Near a Flat Plate," *ASME Journal of Tribology*, 113, pp. 355-360.
- [49] Chen, J.S. and Lin, C., 2005, "Axisymmetrical Snapping of a Spinning Nonflat Disk," *Journal of Applied Mechanics*, 72(6), pp. 879-886.

- [50] Chen, J.S. and Chang, Y., 2007, "On the Unsymmetrical Deformation and Reverse Snapping of a Spinning Non-Flat Disk," *International Journal of Non-Linear Mechanics*, 42(8), pp. 1000-1009.
- [51] Tobias, S.A., and Arnold, R.N., 1957, "The Influence of Dynamical Imperfections on Vibration of Rotating Disks," *Institution of Mechanical Engineers, Proceedings* 171, pp. 669-690.
- [52] Tobias, S.A., 1958, "Non-Linear Forced Vibrations of Circular Discs: an Experimental Investigation," *Engineering*, 186, pp. 51-56.
- [53] Thomas, O., Touze, C., and Chaigne, A., 2003, "Asymmetric Non-Linear Forced Vibrations of Free-Edge Circular Plates. Part II: Experiments," *Journal of Sound and Vibration*, 265, pp. 1075-1101.
- [54] Raman, A., and Mote, C.D., 2001, "Experimental Studies on the Non-Linear Oscillations of Imperfect Circular Disks Spinning Near Critical Speed," *International Journal of Non-Linear Mechanics*, 36, pp. 291-305.
- [55] D'Angelo, C., and Mote, C.D., 1993, "Aerodynamically Excited Vibration and Flutter of a Thin Disk Rotating at Supercritical Speed," *Journal of Sound and Vibration*, 168, pp. 15-30.
- [56] Raman, A., Hansen, M.H., and Mote, C.D., 2002, "A Note on the Post-Flutter Dynamics of a Rotating Disk," *Journal of Applied Mechanics*, 69, pp. 864-866 .
- [57] Kang, N, and Raman, A., 2006, "Vibrations and Stability of a Flexible Disk Rotating in a Gas-Filled Enclosure-Part 2: Experimental Study," *Journal of Sound and Vibration*, 296, pp. 676-68.
- [58] Jana, A., and Raman, A., 2005, "Nonlinear Aeroelastic Flutter Phenomena of a Flexible Disk Rotating in an Unbounded Fluid," *Journal of Fluids and Structures*, 20, pp. 993-1006
- [59] Jana, A., and Raman, A., 2005, "Nonlinear Dynamics of a Flexible Spinning Disc Coupled to a Precompressed Spring," *Nonlinear Dynamics*, 40, pp. 1-20.
- [60] Chen, J.S., 1999, "Steady State Deflection of a Circular Plate Rotating Near its Critical Speed," *Journal of Applied Mechanics*, 66, pp. 1015-1017.
- [61] Nayfeh, A. H., Jilani, A., and Manzione, P., 2001, "Transverse Vibrations of a Centrally Clamped Rotating Circular Disk," *Nonlinear Dynamics*, 26, pp. 163-178.

- [62] Chen, J.S., 2001, "On the Internal Resonance of a Spinning Disk Under Space-Fixed Pulsating Edge Loads," *Journal of Applied Mechanics*, 68, pp. 854-859.
- [63] Touze, C., Thomas, O., and Chaigne, A., 2002, "Asymmetric Non-linear Forced Vibrations of Free-Edge Circular Plates. Part 1: Theory," *Journal of Sound and Vibration*, 258, pp. 649-676.
- [64] Yang, L., and Hutton, S.G., 1998, "Nonlinear Vibrations of Elastically-Constrained Rotating Discs," *Journal of Vibration and Acoustics*, 120, pp. 475-483.
- [65] Luo, A.C.J., and Mote, C.D., 2000, "Nonlinear Vibration of Rotating Thin Disks", *Journal of Vibration and Acoustics*," 122, pp. 376-383.
- [66] Arafat, H.N., and Nayfeh, A.H., 2004, "Natural Frequencies of Heated Annular and Circular Plates," *International Journal of Solids and Structures*, 41, pp. 3031-3051.
- [67] Arafat, H. N. and Nayfeh, A. H., 2004, "Modal Interactions in the Vibrations of a Heated Annular Plate," *International Journal of Non-Linear Mechanics*, 39(10), pp. 1671-1685.
- [68] Arafat, H.N., and Nayfeh, A.H., 2004, "Combination Internal Resonances in Heated Annular Plates," *Nonlinear Dynamics*, 37, pp. 285-306.
- [69] Chen, J., and Hua, C., 2004, "On the Secondary Resonance of a Spinning Disk Under Space-Fixed Excitations," *ASME Journal of Vibration and Acoustics*, 126, pp. 422-429.
- [70] Heo, J.W., Chung, J., and Choi, K., 2003, "Dynamic Time Responses of a Flexible Spinning Disk Misaligned with the Axis of Rotation," *Journal of Sound and Vibration*, 262, pp. 25-44.
- [71] Raman, A., and Mote, C.D., 2001, "Effects of Imperfection on the Non-Linear Oscillations of Circular Plates Spinning Near Critical Speed," *International Journal of Non-Linear Mechanics*, 36, pp. 261-289.
- [72] Manzione, P., and Nayfeh, A.H., 2001, "Instability Mechanisms of a Centrally Clamped Rotating Circular Disk Under a Space-Fixed Spring-Mass-Dashpot System," *Journal of Vibration and Control*, 7, pp. 1013-1034.
- [73] Jalali, M.A., and Angoshtari, A., 2006, "Phase Space Structure of Spinning Disks," *International Journal of Non-Linear Mechanics*, 41, pp. 726-35.

Chapter 2- On the Effects of Rigid Body Translational Mode*

2.1. Introduction

Elastically constrained rotating circular disks constitute components in many important engineering applications. In some of these applications the disks may be elastically constrained and have rigid body degrees of freedom. In these cases rigid body degrees of freedom need to be considered in the analysis of the vibration response. Hutton, Chonan, and Lehmann [1] studied the dynamic response characteristics of rotating circular disks when subjected to the effect of forces produced by stationary spring guides. Mote [2] studied the effect of a collar (which was allowed to move freely on the arbor) on the stability of a guided rotating disk. Price [3] studied the dynamics of plates with clamped-free boundary conditions and studied the effect of a rigid body translational mode on the dynamic response of rotating plates. Tian and Hutton [4] developed an analytical model for modeling wood cutting of circular saws in order to understand the mechanism of washboarding. Jia [5] studied the vibration characteristics of a disk which has initial non-flatness.

Jana and Raman [6] investigated the nonlinear dynamics of a flexible spinning disk coupled to a precompressed spring. They studied large amplitude wave motions and their stability using the averaging method. Nayfeh, Jilani and Manzione [7] used the method of multiple scales to investigate the transverse nonlinear vibrations of a centrally clamped rotating circular disk. Yang and Hutton [8] used a polynomial expansion for the approximation function in the Galerkin method to solve the nonlinear equations of motion for rotating thin disks.

* A version of this chapter has been accepted for publication. Khorasany, R.M.H., and Hutton, S.G., 2010, “ An Analytical Study on the Effect of Rigid Body Translational Degree of Freedom on the Vibration Characteristics of Elastically Constrained Rotating Disks”, International Journal of Mechanical Sciences.

Among all of the works that have been done so far in this subject, only a few of them have been concerned with the effect of rigid body degrees of freedom on the stability characteristics of spinning disks. Chen and Wong [9] used finite element analysis to study the effect of evenly fixed spaced springs on the divergence instability of rotating disks which have translation degrees of freedom. Yang [10] studied the transverse vibration of a disk with free-free boundary conditions and studied the effect of translational and tilting rigid body degrees of freedom. He used numerical techniques to study the effect of rigid body degrees of freedom on the vibrations of a spinning disk.

In this chapter, previous numerical work is generalized by the use of an analytical approach to investigate the stability characteristics of an elastically constrained spinning disk with one space fixed spring, around a critical speed. In order to do so, a three mode approximation is used around the critical speed and it is shown that the disk is neutrally stable at its critical speed. It is also confirmed that the critical speed does not change with changing the spring stiffness and it is the same as for the unguided disk

For a spinning disk, the rigid body translational mode may interact with a forward, a backward or a reflected wave. An analytical approach is taken to investigate the stability characteristics of the guided disk for each of the above three types of interaction.

2.2. Linear Equations of Motion

A flexible spinning disk having a rigid body translational degree of freedom is considered. The inner radius of the disk is “a”, its outer radius is “b” and its thickness is ‘h’. The disk is assumed to be elastically constrained with one space fixed spring. The disk is rotating with an angular speed Ω about the z axis and is free to have rigid body translation along the z axis. Figure 2. 1 presents a schematic diagram of the annular spinning disk.

In this chapter, we assume that the disk is capable of having rigid body translation. A flexible disk without having any rigid body degrees of freedom has three components of acceleration in the z direction: bending, Coriolis and centrifugal acceleration. When rigid body translation is added to the system, one more component of acceleration (rigid body translational acceleration, \ddot{Z}_0) should be taken into account. This component of acceleration is uniform in the disk domain. By simply adding this component of

acceleration to the left hand side of the equation of motion (Hutton et. al. [1]), one can find the governing equation for the bending of the spinning disk (Eq. (2.1)). It has to be noted that we assume that there is no lateral external force acting on the disk.

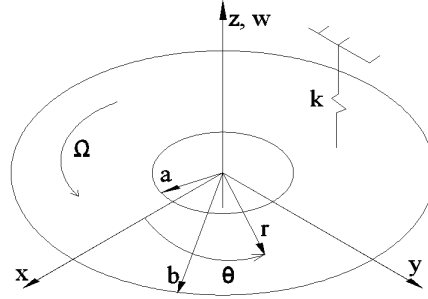


Figure 2. 1. A guided rotating disk with rigid body degrees of freedom

In addition to the governing equation for the disk bending, we need one more equation which governs the rigid body translational motion in the z direction. The same components of acceleration that have been stated above are potentially present in the governing equation for the rigid body motion and one has to find the net effect of them on the rigid body motion. It has to be emphasized that that the Coriolis and centrifugal accelerations only exist for the preferential modes. Therefore, the net effect of these two terms in the governing equation of rigid body motion in the z direction is zero. The only two remaining acceleration components are: rigid body acceleration and bending acceleration. One has to integrate the bending acceleration over the disk area to find the effect of this component of acceleration on the motion of the spinning disk in the z direction. Since the disk is elastically constrained, the spring exerts a force in the z direction that appears in both of the governing equations. Therefore, the non-dimensionalized equations of motion for an elastically constrained flexible spinning disk having rigid body translational degrees of freedom are obtained to be

$$\frac{\partial^2 w}{\partial t^2} + 2\Omega \frac{\partial^2 w}{\partial \theta \partial t} + \Omega^2 \frac{\partial^2 w}{\partial \theta^2} + \nabla^4 w - \frac{\Omega^2}{b^2} (C_{rr} w_{,rr} + C_r w_{,r} + C_{\theta\theta} w_{,\theta\theta}) + \ddot{Z}_0 = -(k/r) \delta(r - r^k) \delta(\theta - \theta^k) [w(r, \theta, t) + Z_0] \quad (2.1)$$

$$A_D \ddot{Z}_0 + \int_0^{2\pi} \int_a^b \frac{\partial^2 w}{\partial t^2} r dr d\theta + k [w(r^k, \theta^k, t) + Z_0] = 0, \quad (2.2)$$

where the relation between the actual parameters and normalized parameters (shown with prime) are

$$r' = \frac{r}{b}, \quad w' = \frac{bw}{h^2}, \quad Z'_0 = \frac{bZ_0}{h^2}, \quad t' = tT, \quad \Omega' = \frac{1}{T}\Omega, \quad k' = \frac{b^4}{D}k, \quad T = \frac{(D/\rho h)^{1/2}}{b^2}.$$

where w is the transverse deflection of the disk, Z_0 is the rigid body translational degree of freedom, ρ is disk density, E is Young's modulus, ν is Poisson's ratio, A_D is the area of the disk, D is the disk rigidity, Ω is the rotation speed, $\delta(\)$ is the Dirac delta function and k is the stiffness of the spring and (r^k, θ^k) is its space fixed polar location in the inertial coordinate system. In the current paper it is assumed that the disk is rigidly fixed in its inner boundary to a collar. The collar is capable of having rigid body translation in the z direction. C_{rr} , C_r and $C_{\theta\theta}$ are constants defining the in-plane stresses due to rotation found from the following equations

$$\begin{aligned} C_{rr} &= C_1 + \frac{C_2}{r^2 b^2} + C_3 r^2 b^2, \\ C_r &= b \frac{C_1}{rb} - \frac{C_2}{r^3 b^3} + 3C_3 r b, \\ C_{\theta\theta} &= b^2 \frac{C_1}{r^2 b^2} - \frac{C_2}{r^4 b^4} + C_4, \end{aligned}$$

where

$$\begin{aligned} C_1 &= \frac{1+\nu}{8} \frac{(\nu-1)a^4 - (3+\nu)b^4}{(\nu-1)a^2 - (1+\nu)b^2}, \\ C_2 &= \frac{1-\nu}{8} a^2 b^2 \frac{(\nu+1)a^2 - (3+\nu)b^2}{(\nu-1)a^2 - (1+\nu)b^2}, \\ C_3 &= -(3+\nu)/8, \\ C_4 &= -(1+3\nu)/8. \end{aligned}$$

2.3. Interaction Between a Backward Traveling Wave and Its Complex Conjugate with Rigid Body Translational Mode

In order to investigate the stability of a guided disk at around its critical speed, a three mode approximation is used here. Let's consider the following approximation for the eigenfunction of the disk at around its critical speed

$$\tilde{w}(r, \theta, t) = \tilde{R}_{mn}^w(r) [c_1^w e^{+im\theta} + c_2^w e^{-im\theta}] + Z_0, \quad (2.3)$$

where i is the imaginary unit ($\sqrt{-1}$), $\tilde{R}_{mn}^w(r)$ is the mode shape in the radial direction of the disk at round its critical speed. $\tilde{R}_{mn}^w(r)e^{+im\theta}$ and $\tilde{R}_{mn}^w(r)e^{-im\theta}$ are the backward and forward traveling waves, respectively, and c_1^w and c_2^w are their associated expansion coefficients, respectively. It is assumed that m is positive. In order to simplify the equation of motion, we assume the natural frequency of the disk without rigid body degrees of freedom in the vicinity of the critical speed and in the inertial frame to be $\tilde{\omega}_{mn}$. Indeed at the critical speed one of the natural frequencies of the system is zero. Therefore using Eq. (2.1) and ignoring the rigid body translation mode we can see that

$$\begin{aligned} \Omega^2 \frac{\partial^2}{\partial \theta^2} + \nabla^4 - \frac{\Omega^2}{b^2} C_{rr} \frac{\partial^2}{\partial r^2} + C_r \frac{\partial}{\partial r} + C_{\theta\theta} \frac{\partial^2}{\partial \theta^2} \tilde{R}_{mn}^w(r) e^{\pm im\theta} \\ = \tilde{\omega}_{mn} (\tilde{\omega}_{mn} \pm 2m\Omega) \tilde{R}_{mn}^w(r) e^{\pm im\theta}. \end{aligned} \quad (2.4)$$

It is assumed that the spring acts at $r=1$ and $\theta=0$ and its stiffness is k . After substituting Eq. (2.3) into Eqs. (2.1) and (2.2) and using the general relation stated in Eq. (2.4) and then utilizing the Galerkin's projection the following coupled linear equations are obtained

$$\begin{aligned} \tilde{M} \ddot{\tilde{x}} + \tilde{G} \dot{\tilde{x}} + \tilde{K} \tilde{x} = 0, \quad (2.5) \\ \tilde{x} = \begin{matrix} c_1^w \\ c_2^w \\ Z_0 \end{matrix}, \quad \tilde{M} = \begin{matrix} 1 & 0 & 0 \\ 0 & 1 & 0 \\ 0 & 0 & A_D \end{matrix}, \quad \tilde{G} = \begin{matrix} 2m\Omega i & 0 & 0 \\ 0 & -2m\Omega i & 0 \\ 0 & 0 & 0 \end{matrix}, \\ \tilde{K} = \begin{matrix} S_{mn} + kR^2 & kR^2 & kR \\ kR^2 & S_{mn} + kR^2 & kR \\ kR & kR & k \end{matrix}, \end{aligned}$$

where k is the stiffness of the spring and $R = \tilde{R}_{mn}^w(1)$. It should be mentioned that the natural frequencies of the two traveling waves interacting at the critical speed are the same but with opposite signs; therefore S_{mn} is the same for both of the interacting traveling waves and equals $\tilde{\omega}_{mn} (\tilde{\omega}_{mn} + 2m\Omega)$. In this equation $\tilde{\omega}_{mn}$ is assumed to be positive at the speed lower than the critical speed and negative for the speeds above the critical speed. If we substitute $e^{\lambda t}$ instead of $\tilde{x}(t)$ in Eq. (2.5), the characteristic equation is:

$$\alpha_1 \lambda^6 + \alpha_2 \lambda^4 + \alpha_3 \lambda^2 + \alpha_4 = 0, \quad (2.6)$$

where

$$\begin{aligned} \alpha_1 &= A_D, \\ \alpha_2 &= A_D(2kR^2 + 2S_{mn} + 4m^2\Omega^2) + k, \\ \alpha_3 &= A_D S_{mn}(2kR^2 + S_{mn}) + 2k(2m^2\Omega^2 + S_{mn}), \\ \alpha_4 &= k S_{mn}^2. \end{aligned}$$

Eq. (2.6) is a third order polynomial equation in terms of λ^2 . Therefore in order to have three distinct roots for λ^2 , the discriminant of Eq. (2.6) should be positive. The discriminant of the above equation is:

$$\Delta = -4\alpha_2^3\alpha_4 + \alpha_2^2\alpha_3^2 - 4\alpha_1\alpha_3^3 + 18\alpha_1\alpha_2\alpha_3\alpha_4 - 27\alpha_1^2\alpha_4^2. \quad (2.7)$$

After substituting $\alpha_1, \alpha_2, \alpha_3$ and α_4 into Eq. (2.7), the discriminant is found to have the following form

$$\Delta = \beta_5 S_{mn}^5 + \beta_4 S_{mn}^4 + \beta_3 S_{mn}^3 + \beta_2 S_{mn}^2 + \beta_1 S_{mn} + \beta_0, \quad (2.8)$$

where

$$\beta_0 = 16m^4\Omega^4k^2 \left[(4R^4A_D^2 + 1 + 4R^2A_D)k^2 + (16R^2A_D^2m^2\Omega^2 - 8m^2\Omega^2A_D)k + 16m^4\Omega^4A_D^2 \right] \quad (2.9a)$$

$$\beta_1 = 8m^2\Omega^2(2 + 8A_D^3R^6 + 16A_D^4R^4 + 10A_DR^2)k^4 + 64m^4\Omega^4(2A_D^2R^2 - 3A_D + 4A_D^3R^4)k^3 + 256m^6\Omega^6A_D^2(A_DR^2 + 2)k^2, \quad (2.9b)$$

$$\beta_2 = 4R^4A_D^2(1 + 4R^4A_D^2 + 4R^2A_D)k^4 + 8m^2\Omega^2A_D(-10R^2A_D + 8R^6A_D^3 - 8R^4A_D^2 - 8)k^3 + 32m^4\Omega^4A_D^2(4R^2A_D^3 + 11 + 8R^4A_D^2)k^2 - 128m^6\Omega^6A_D^3k, \quad (2.9c)$$

$$\beta_3 = 8R^4A_D^3(2R^2A_D - 1)k^3 + 16m^2\Omega^2A_D^2(6 + 8R^4A_D^2 - 5R^2A_D)k^2 + 64m^4\Omega^4A_D^3(-3 + R^2A_D), \quad (2.9d)$$

$$\beta_4 = 4R^4A_D^4k^2 + 8m^2\Omega^2A_D^3(10R^2A_D - 8)k + 16m^4\Omega^4A_D^4, \quad (2.9e)$$

$$\beta_5 = 16m^2\Omega^2A_D^4. \quad (2.9f)$$

In a very close vicinity of the critical speed, $\tilde{\omega}_{mn}$ is very close to zero. Therefore in the vicinity of critical speed we can conclude that $S_{mn} \ll 1$. As a result, it may be concluded from Eq. (2.8) that the only term which affects the sign of the discriminant in the vicinity of the critical speed is β_0 . From Eq. (2.9a) it can be seen that β_0 is a fourth order equation in terms of k . As shown in this equation, k^2 can be factored out and these

remains a second order polynomial equation in terms of k . So β_0 can be written as $16m^4\Omega^4k^2\beta'_0$ where

$$\beta'_0 = (4R^4A_D^2 + 1 + 4R^2A_D)k^2 + (16R^2A_D^2m^2\Omega^2 - 8m^2\Omega^2A_D)k + 16m^4\Omega^4A_D^2 \quad (2.10)$$

Therefore, the sign of the discriminant in the close vicinity of the critical speed depends upon the sign of β'_0 . β'_0 is a second order polynomial equation in terms of k . If we put $\beta'_0 = 0$, the two roots of the equation for the stiffness are obtained to be

$$k_{1,2} = -\frac{4(2A_DR^2 - 1 \pm 2R\sqrt{-2A_D})Am^2\Omega^2}{1 + 4R^4A_D^2 + 4R^2A_D}. \quad (2.11)$$

Since A_D is always positive, from Eq. (2.11) it can be seen that the numerator is imaginary. Therefore, there is no real root for k which can make β' to be zero, based on Eq. (2.10). The coefficient of the second order term (k^2) in Eq. (2.11) is positive. Therefore it can be concluded that β'_0 is always positive in the close vicinity of the critical speed for any value of k . As a result of that the discriminant of Eq. (2.6) is always positive. This implies that the characteristics equation has always three real roots for λ^2 in the vicinity of the critical speed. In a close vicinity of the critical speed $\alpha_1, \alpha_2, \alpha_3$ and α_4 are always positive for any value of k . This means that the three real roots for λ^2 must be negative which implies that all the eigenvalues at around the critical speed are imaginary. Indeed, the guided disk does not experience divergence type instability in the vicinity of the critical speed. If we substitute $\tilde{\omega}_{mn} = 0$ into Eq. (2.6) we can see that one of the roots for λ is zero which implies that by adding a spring to the system the critical speed does not change and remains the same as the one for an unguided disk. In order to investigate this issue numerically, a disk made of steel with clamped-free boundary conditions is considered. It is assumed that $E = 2e11 N/m^2, \nu = 0.3, \rho = 7800 kg/m^3, \eta = a/b = 0.3529, b = 0.2159 m, h = 1.27 mm$. In Figure 2. 2 comparisons between the normalized natural frequencies of the guided disk when $k = 0.057$ and $k = 2.85$ (broken lines) with the unguided disk (solid lines) are carried out. It should be emphasized that $k = 0.057$ and $k = 2.85$ are normalized stiffness and the actual corresponding stiffness are

10^3 N/m and $5 \times 10^4 \text{ N/m}$, respectively. In this figures (m,n)b means the backward traveling wave of the (m,n) mode and ‘RB’ stands for the rigid body translational mode. It can be seen that by adding a spring to the system, at a critical speed of the unguided disk, divergence instability is not induced. In fact, the guided disk has the same critical speeds as the unguided disk.

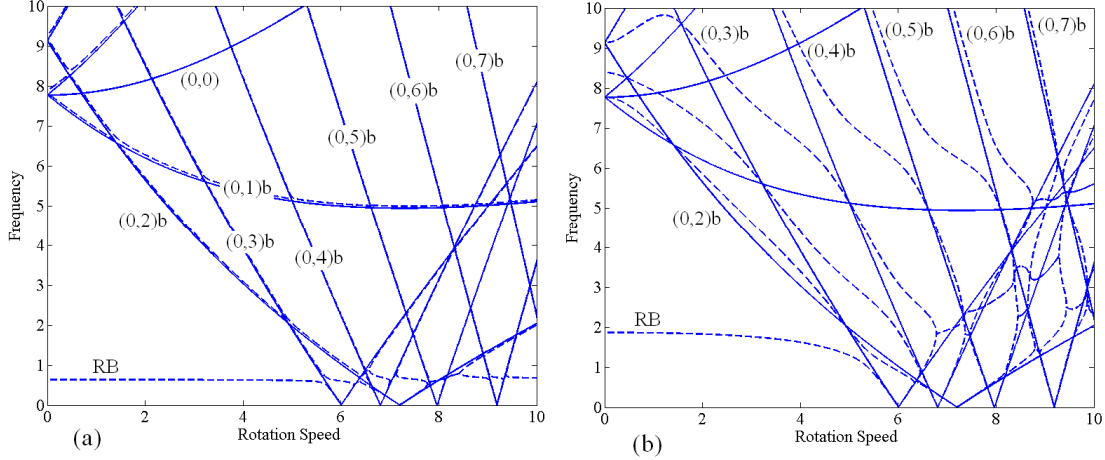


Figure 2. 2. Normalized natural frequencies of the guided disk (shown with the broken lines) versus normalized speed when (a) $k = 0.057$ and (b) $k = 2.85$. The solid lines show the normalized natural frequencies of the unguided disk

2.4. Interaction Between a Forward or Backward or Reflected Traveling Wave with Rigid Body Translational Mode

Another interesting issue that we can look at is the interaction of rigid body translational mode with another bending mode at speeds other than the critical speed. Generally we have three types of interactions and they happen when the rigid body translational mode interacts with a forward, backward or a reflected traveling wave mode. In order to investigate these three types of interactions, we can use the following approximation for the eigenfunction of the rotating disk:

$$\tilde{w}(r, \theta, t) = c_1^w \tilde{R}_m^w(r) e^{im\theta} + Z_0, \quad (2.12)$$

where $\tilde{R}_m^w(r) e^{im\theta}$ is the backward or forward traveling wave component (depending on the sign of m) and c_1^w is its associated expansion coefficient. When m is negative, the assumed mode is either a forward or reflected wave and when m is positive, the assumed

mode is a backward wave mode. After substituting Eq. (2.12) into Eqs. (2.1) and (2.2) and utilizing the Galerkin's projection the following coupled linear equations are obtained

$$\tilde{M} \ddot{\tilde{x}} + \tilde{G} \dot{\tilde{x}} + \tilde{K} \tilde{x} = 0, \quad (2.13)$$

where

$$\tilde{x} = \begin{pmatrix} \tilde{c}_1^w \\ Z \end{pmatrix}, \quad \tilde{M} = \begin{pmatrix} 1 & 0 \\ 0 & A_D \end{pmatrix}, \quad \tilde{G} = \begin{pmatrix} 2m\Omega i & 0 \\ 0 & 0 \end{pmatrix},$$

$$\tilde{K} = \begin{pmatrix} S_{mn} + kR^2 & kR \\ kR & k \end{pmatrix},$$

where S_{mn} equals $\tilde{\omega}_{mn}(\tilde{\omega}_{mn} + 2m\Omega)$. It is important to note that S_{mn} is less than zero when we deal with a reflected wave and greater than zero when we deal with a backward or forward traveling wave. After substitution of $\tilde{x} = Xe^{\lambda t}$ into Eq. (2.13), the following characteristic equation is obtained

$$A_D \lambda^4 + 2im\Omega A_D \lambda^3 + (A_D S_{mn} + A_D kR^2 + k) \lambda^2 + 2im\Omega k \lambda + S_{mn} k = 0. \quad (2.14)$$

We assume that $\lambda = i\omega$ where ω is a real number. After substitution of $\lambda = i\omega$ into Eq. (2.14), the following characteristics equation is obtained

$$f(\omega, k) = A_D \omega^4 + 2m\Omega A_D \omega^3 - (A_D S_{mn} + A_D kR^2 + k) \omega^2 - 2m\Omega k \omega + S_{mn} k = 0 \quad (2.15)$$

For a backward or forward wave it may be noted that $S_{mn} k$ is always positive. The general shape of $f(\omega, k)$ for any given values of k using the characteristics of a backward or forward traveling wave is shown in Figure 2. 3. As it can be seen from this figure, when $\omega = 0$, $f(\omega, k)$ is greater than zero. In order to show that when a backward or forward traveling wave interacts with the rigid body translational mode flutter type instability is not induced, we have to prove that Eq. (15) has always four real roots for a backward or forward wave.

At first consider a backward traveling wave. If we substitute $\omega_1 = -\tilde{\omega}_{mn} - 2m\Omega$ into Eq. (2.15), the following expression is found

$$f(-\tilde{\omega}_{mn} - 2m\Omega, k) = -kR^2 A_D (\tilde{\omega}_{mn} + 2m\Omega)^2. \quad (2.16)$$

Also if we substitute $\omega_2 = \tilde{\omega}_{mn}$ into Eq. (2.15), the following expression is found

$$f(\tilde{\omega}_{mn}, k) = -kR^2 A_D (\tilde{\omega}_{mn})^2. \quad (2.17)$$

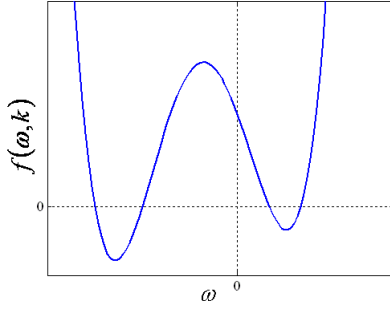


Figure 2. 3. A general shape for $f(\omega, k)$ using the characteristics of a backward or forward traveling wave

From Eqs. (2.16) and (2.17) it can be seen that at $\omega_1 = -\tilde{\omega}_{mn} - 2m\Omega$ and $\omega_2 = \tilde{\omega}_{mn}$, $f(\omega, k)$ is always negative for a backward traveling wave. For a backward or forward traveling wave, ω_2 is always positive. For a backward traveling wave ω_1 is always negative. For a forward traveling wave, ω_1 is negative for the speeds less than the critical speed and for the speeds above the critical speed it is positive. Therefore, for a forward traveling wave we use $\omega_3 = -\sqrt{k/A_D}$, instead of ω_1 , which is always a negative real value. If we substitute ω_3 into Eq. (2.15), the following expression is obtained

$$f(-\sqrt{k/A_D}, k) = -kR^2. \quad (2.18)$$

This equation implies that for a backward or forward traveling wave, there always exists a point in the left and right hand side of the vertical axis (Figure 2. 3) at which $f(\omega, k)$ is less than zero. Also in order to show that the plotted graph (Figure 2. 3) is a general shape of $f(\omega, k)$ for a backward or forward traveling wave, we also have to show that $f(\omega, k)$ has two inflection points. If we differentiate Eq. (2.15) with respect to ω , the following equation is obtained

$$\frac{\partial^2 f}{\partial \omega^2} = 12A_D\omega^2 + 12m\Omega A_D\omega - 2(A_D S_{mn} + A_D kR^2 + k). \quad (2.19)$$

Eq. (2.19) is a second order polynomial in terms of ω . Since the coefficients of the second and zero order terms have opposite signs, therefore the discriminant of the above equation is always greater than zero. As a result of that, Eq. (2.15) always has two inflection points. Having two inflection points for $f(\omega, k)$ implies that this function always has two local minima and one local maximum. Therefore based on the above

reasonings, Figure 2. 3 is a general shape of $f(\omega, k)$ for a backward or forward traveling wave.

Finally since $f(\omega, k)$ always has two local minima and one local maximum and also since this function is positive at $\omega = 0$ and negative at $\omega = \omega_1$ and $\omega = \omega_2$ for a backward wave (and negative at $\omega = \omega_1$ and $\omega = \omega_3$ for a forward traveling wave) ; it can be concluded that this function always has four real roots. Two of the real roots are positive and the other two are negative values. This implies that the interaction between the rigid body translational mode and a backward or forward traveling wave does not induce flutter type instability.

When the rigid body translational mode interacts with a reflected traveling wave mode, the situation is different and speed dependent. As was mentioned above, for a reflected traveling wave, S_{mn} is negative. Eq. (2.15) can be decomposed into two parts: the first part which does not depend upon the spring stiffness and the second part which depends upon the spring stiffness. Therefore we can write Eq. (2.15) in the following from

$$f(\omega, k) = f_1(\omega, k) + f_2(\omega, k), \quad (2.20)$$

where

$$\begin{aligned} f_1(\omega, k) &= A_D \omega^4 + 2m\Omega A_D \omega^3 - A_D S_{mn} \omega^2, \\ f_2(\omega, k) &= -(A_D k R^2 + k) \omega^2 - 2m\Omega k \omega + S_{mn} k. \end{aligned}$$

$f_2(\omega, k)$ is a second order polynomial equation in terms of ω . The discriminant of this equation ($f_2(\omega, k)$) is found to be

$$\Delta = 4k^2 [m^2 \Omega^2 + (A_D R^2 + 1) S_{mn}] \quad (2.21)$$

As can be seen from Eq. (2.21), the sign of the discriminant does not depend upon the stiffness of the spring. The sign only depends upon the speed, the mode itself and the disk characteristics such as area and also the radial position of the spring. Since S_{mn} is negative for a reflected wave, the two roots of $f_1(\omega, k)$ are positive real values and the other two roots are zero. There are two possibilities: either the discriminant of $f_2(\omega, k)$ is negative or positive. As a first step we assume that the discriminant of $f_2(\omega, k)$ is positive. In this case $f_2(\omega, k)$ has two real solutions for ω for any given value of spring

stiffness and both of them are negative real values. Figure 2. 4 shows a typical plot for $f_1(\omega, k)$ and $f_2(\omega, k)$ (using Eqs. (2.16) and (2.17) and the fact that ω_1 and ω_2 are the real roots of $f_1(\omega, k)$). By increasing the stiffness of the spring, the local maxima of $f_2(\omega, k)$ moves upward. This figure shows the plot of $f_2(\omega, k)$ for a relatively small and large value of spring stiffness (k). From this graph it can be seen that for a sufficiently small value of spring stiffness, $f(\omega, k)$ has four real roots of which three of them are positive and the fourth one is negative. If the stiffness is further increased to a certain level (e.g. stiffness is equal to k_1^-), a situation is reached at which $f(\omega, k)$ only intersects the horizontal axis at two points. This case can be qualitatively verified from Figure 2. 4 when the spring stiffness is relatively high. This point is the starting point of flutter type instability. It should be noted that k_1^- depends upon the mode, disk characteristics and rotation speed.

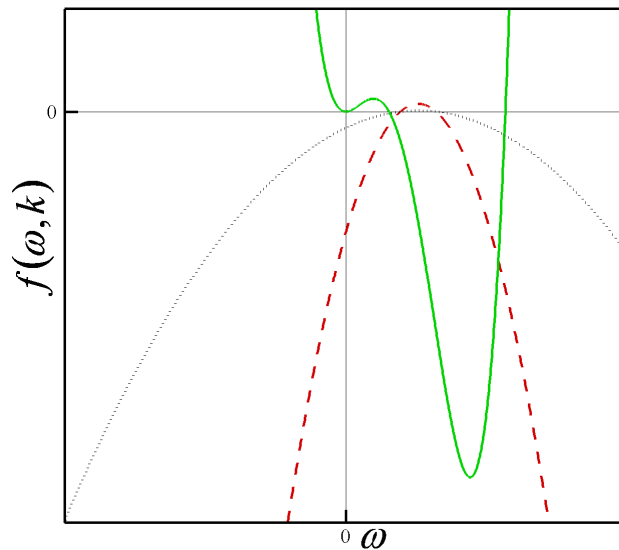


Figure 2. 4. A typical plot of $f_1(\omega, k)$ (solid line) and $f_2(\omega, k)$ for a relatively small (dotted line) and large (dashed line) value of k when the discriminant of $f_2(\omega, k)$ is positive

Since the discriminant of $f_2(\omega, k)$ is assumed to be positive, it can be concluded that the maximum value of $f_2(\omega, k)$ for any given value of spring stiffness is always positive. So if the stiffness is further increased (e.g. stiffness is equal to k_1^+) a situation is reached in which $f(\omega, k)$ starts to have four real roots again. In this case again, three of the real

roots are positive real values and the last one is negative. This stiffness (k_1^+) corresponds to the stiffness for which the flutter type instability disappears for a given rotation speed. Therefore at any speed that the discriminant of $f_2(\omega, k)$ is positive when $k_1^- < k < k_1^+$, the interaction of the backward wave and rigid body translational does not produce flutter type instability. Determination of the explicit values for k_1^+ and k_1^- is difficult.

Another possible situation is that the discriminant of $f_2(\omega, k)$ is less than zero. In this case $f_2(\omega, k)$ does not have any real roots. Also for any given value of the spring stiffness, $f_2(\omega, k)$ is always negative as shown in Figure 2. 5. One of the major differences between this situation and the previous situation is that $f_2(\omega, k)$ always lies below the horizontal axis for a nonzero given value of spring stiffness. In this case, when the spring stiffness is relatively small, $f(\omega, k)$ has four real roots of which three of them are positive and the fourth one is negative.

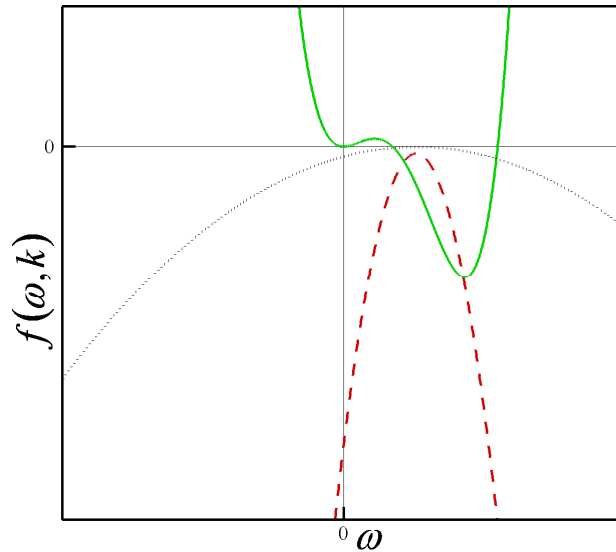


Figure 2. 5. A typical plot of $f_1(\omega, k)$ (solid line) and $f_2(\omega, k)$ for a relatively small (dotted line) and large (dashed line) value of k when the discriminant of $f_2(\omega, k)$ is negative

From Figure 2. 5 it can be seen that by increasing the stiffness of the spring to a certain level (k_2^-), a situation is reached at which $f(\omega, k)$ does not have four real roots any more. In this case, a flutter type instability is induced due to interaction between the rigid body mode and the reflected wave. From Figure 2. 5, it may be noted that by further

increasing the spring stiffness the flutter type instability does not disappear. Therefore, for any $k > k_2^-$, the disk loses its stability due to flutter type instability.

Figure 2. 6 shows non-dimensional natural frequencies (measured by a stationary observer) plotted against non-dimensional speed of the spinning disk with clamped-free boundary conditions for different levels of spring stiffness. The spring stiffnesses in this figure are normalized. It is assumed that the disk has a rigid body translational degree of freedom, as explained previously.

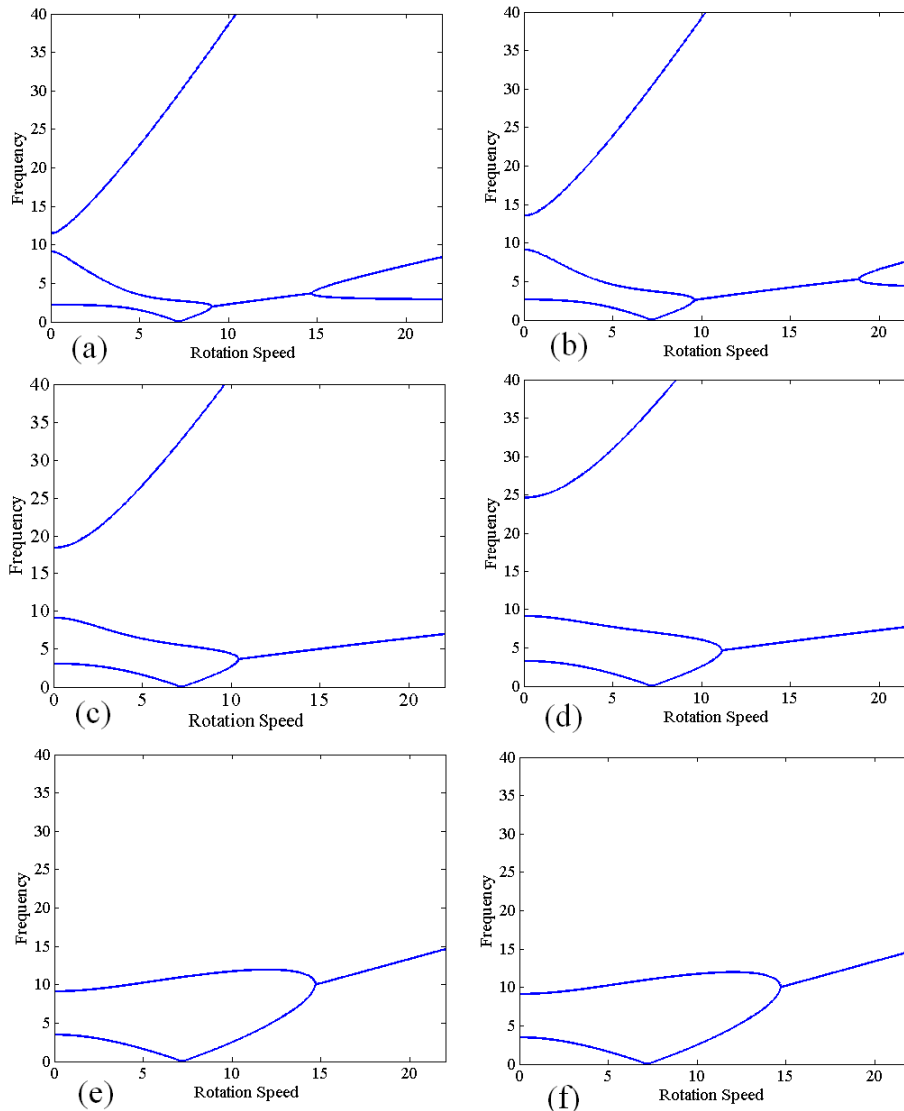


Figure 2. 6. The interaction between the (0,2) mode of the clamped disk with rigid body translational mode when (a) $k = 1$, (b) $k = 2$, (c) $k = 5$, (d) $k = 10$, (e) $k = 10^4$ and (f) $k = 10^6$

In Figure 2. 6, a two-mode approximation is used and the interaction between the (0,2) bending mode and the rigid body translation mode is investigated. The response depends upon the relationship between the magnitude of the spring stiffness and the bending stiffness of the (0,2) mode. For sufficiently high values of k the spring behaves as a rigid support. It can be seen that when the reflected wave of (0,2) mode interacts with the rigid body translational mode, flutter type instability is induced. It may be noted that as the stiffness increases up to $k = 10^4$, the region of flutter type instability moves toward higher speeds.

By a comparison between Figure 2. 6e and Figure 2. 6f it may be noted that although the spring stiffness is increased above 10^4 the response does not change and thus the spring acts as a rigid support and the starting point of flutter type instability is the same for both of these plots ($k = 10^4$ and $k = 10^6$) and occurs at $\Omega = 14.72$. This speed corresponds to the starting region of speeds at which the discriminant of $f_2(\omega, k)$ is negative. As can be seen from these figure, when the stiffness changes from $k = 10^4$ to $k = 10^6$, the starting point of flutter type instability regions does not change. Also for any speed greater than $\Omega = 14.72$, there is a threshold of the stiffness such that if the spring stiffness exceeds this threshold, the disk loses its stability due to flutter instability and never disappears. This flutter instability is induced due to interaction between the rigid body translational mode and the reflected wave of (0,2) mode. It is difficult to find an explicit value for the speed at which the gradient of $f_2(\omega, k)$ starts to be negative and also to find the stiffness threshold that was discussed above.

2.5. Conclusions

Using analytical calculations, the effect of rigid body translational motion on the stability characteristics of an elastically constrained disk with only one space fixed spring was studied. It was shown that because of the effect of the rigid body translational degree of freedom, divergence instability does not take place. In fact, it was shown that in this case the guided disk still has the same critical speeds as the unguided disk. This result corresponds to the fact that the bending wave speed in the disk is not altered by the presence of a point constraint.

Using analytical calculations, it was shown that the interaction of a forward or backward traveling wave with the rigid body translational mode does not induce flutter type instability. When the rigid body translational mode interacts with a reflected traveling wave, there are two possibilities: the discriminant of $f_2(\omega, k)$ is (i) positive or (ii) negative. It was shown that in the first case (discriminant is positive) there is a range of spring stiffness ($k_1^- < k < k_1^+$) for which flutter type instability will be induced. In the second case (discriminant is negative), if the spring stiffness exceeds a certain value ($k > k_2^-$), then flutter instability will be induced and never disappear as the spring stiffness is increased.

2.6. References

- [1] Hutton, S.G., Chonan, S., and Lehmann, B.F., 1987, "Dynamic Response of a Guided Circular Saw," *Journal of Sound and Vibration*, 112, pp. 527-539.
- [2] Mote, C.D., 1977, "Moving Load Stability of a Circular Plate on a Floating Central Collar," *Journal of Acoustical Society of America*, 61, pp. 439-447.
- [3] Price, K.B., 1987, "Analysis of the Dynamics of Guided Rotating Free Center Plates," Ph.D. Dissertation, University of California, Berkeley.
- [4] Tian, J.F., and Hutton, S.G., 2001, "Cutting-Induced Vibration in Circular Saws," *Journal of Sound and Vibration*, 242, pp. 907-922.
- [5] Jia, H. S., 2000, "Analysis of Transverse Runout in Rotating Flexible Disks by Using Galerkin's Method," *International Journal of Mechanical Sciences*, 42, pp. 237-248.
- [6] Jana, A., and Raman, A., 2005, "Nonlinear Dynamics of a Flexible Spinning Disc Coupled to a Precompressed Spring," *Nonlinear Dynamics*, 40, pp. 1-20.
- [7] Nayfeh, A. H., Jilani, A., and Manzione, P., 2001, "Transverse Vibrations of a Centrally Clamped Rotating Circular Disk," *Nonlinear Dynamics*, 26, pp. 163-178.
- [8] Yang, L., and Hutton, S.G., 1998, "Nonlinear Vibrations of Elastically-Constrained Rotating Discs," *Journal of Vibration and Acoustics*, 120, pp. 475-483.
- [9] Chen, J.S., and Wong, C.C., 1995, "Divergence Instability of a Spinning Disk with Axial Spindle Displacement in Contact With Evenly Spaced Stationary Springs," *Journal of Applied Mechanics*, 62, pp. 544-547.
- [10] Yang, S.M., 1993, "Vibration of a Spinning Annular Disk with Coupled Rigid-Body Motion," *Journal of Vibration and Acoustics*, 115, pp. 159-164.